



**HAL**  
open science

# PHYSICS-BASED BALANCING DOMAIN DECOMPOSITION BY CONSTRAINTS FOR HETEROGENEOUS PROBLEMS

Santiago Badia, Hieu Nguyen

► **To cite this version:**

Santiago Badia, Hieu Nguyen. PHYSICS-BASED BALANCING DOMAIN DECOMPOSITION BY CONSTRAINTS FOR HETEROGENEOUS PROBLEMS. 2016. hal-01337968v1

**HAL Id: hal-01337968**

**<https://hal.science/hal-01337968v1>**

Preprint submitted on 27 Jun 2016 (v1), last revised 27 Nov 2018 (v5)

**HAL** is a multi-disciplinary open access archive for the deposit and dissemination of scientific research documents, whether they are published or not. The documents may come from teaching and research institutions in France or abroad, or from public or private research centers.

L'archive ouverte pluridisciplinaire **HAL**, est destinée au dépôt et à la diffusion de documents scientifiques de niveau recherche, publiés ou non, émanant des établissements d'enseignement et de recherche français ou étrangers, des laboratoires publics ou privés.

1     **PHYSICS-BASED BALANCING DOMAIN DECOMPOSITION BY**  
2     **CONSTRAINTS FOR HETEROGENEOUS PROBLEMS \***

3                     SANTIAGO BADIA<sup>†‡</sup> AND HIEU NGUYEN<sup>‡</sup>

4     **Abstract.** In this work, we present a balancing domain decomposition by constraints method  
5 based on an aggregation of elements depending on the physical coefficients. Instead of imposing  
6 constraints on purely geometrical objects (faces, edges, and vertices) of the partition interface, we use  
7 interface objects (subfaces, subedges, and vertices) determined by the variation of the coefficients.  
8 The new method is easy to implement and does not require to solve any eigenvalue or auxiliary  
9 problem. When the physical coefficient in each object is constant at every subdomain containing the  
10 object, we can show both theoretically and numerically that the condition number does not depend  
11 on the contrast of the coefficient. The constant coefficient condition is possible for multi-material  
12 problems. However, for heterogeneous problems with coefficient varying across a wide spectrum of  
13 values in a small spatial scale, such restriction might result in too many objects (a large coarse  
14 problem). In this case, we propose a relaxed version of the method where we only require that the  
15 maximal contrast of the physical coefficient in each object is smaller than a predefined threshold.  
16 The threshold can be chosen so that the condition number is reasonably small while the size of the  
17 coarse problem is not too large. An extensive set of numerical experiments is provided to support  
18 our findings.

19     **Key words.** BDDC, heterogeneous problem, adaptive coarse space, parallel solver, parallel  
20 preconditioner

21     **AMS subject classifications.** 65N55, 65N22, 65F08

22     **1. Introduction.** Many realistic simulations in science and engineering, such  
23 as subsurface flow simulations in a nuclear waste repository or in an oil reservoir, or  
24 heat conduction in composites, involve heterogeneous materials. The linear systems  
25 resulting from the discretization of these problems are hard to solve. The use of direct  
26 solvers at a sufficiently fine scale can be prohibitively expensive, even with modern  
27 supercomputers, due to their high complexity and scalability issues. In addition, the  
28 high contrast of the physical properties significantly increases the condition number  
29 of the resulting linear systems, posing great challenges for iterative solvers. In this  
30 work, we will focus on developing a domain decomposition (DD) preconditioner that  
31 is robust with the variation of the coefficients of the PDEs. For a different but related  
32 approach, to find reasonably accurate heterogeneous solution on a coarse mesh, we  
33 refer the interested readers to [19, 1] and references therein.

34     DD is one of the most popular approaches to solve large-scale problems on parallel  
35 supercomputers. It splits a problem into weakly coupled subproblems on smaller  
36 subdomains and use parallel local solutions on these subdomains to form a parallel  
37 preconditioner for the original problem [50, 41]. In DD, the coarse space plays an  
38 important role in achieving scalability as well as robustness w.r.t variations in the  
39 coefficient. Many early DD methods, such as those in [11, 18, 17, 31, 53], work  
40 for heterogeneous problems when the subdomain partition is a geometric coarse grid  
41 that resolves the discontinuities in the properties of the media. This is a strong  
42 requirement, since the properties of the media might have complicated variations

---

<sup>†</sup>Universitat Politècnica de Catalunya, Jordi Girona 1-3, Edifici C1, 08034 Barcelona, Spain.

<sup>‡</sup>CIMNE – Centre Internacional de Mètodes Numèrics en Enginyeria, Parc Mediterrani de la  
Tecnologia, UPC, Esteve Terradas 5, 08860 Castelldefels, Spain ({sbadia,hnguyen}@cimne.upc.edu).

\*This work has been funded by the European Research Council under the FP7 Program Ideas  
through the Starting Grant No. 258443 - COMFUS: Computational Methods for Fusion Technology  
and the FP7 NUMEXAS project under grant agreement 611636. S. Badia gratefully acknowledges the  
support received from the Catalan Government through the ICREA Acadèmia Research Program.

43 on many scales and be difficult to capture by a geometric coarse grid. Further, it  
 44 is impractical, since it would not lead to load-balanced partitions with a reduced  
 45 interface.

46 Recently, there have been works on coarse grids that do not resolve the hetero-  
 47 geneity in the media [25, 45, 25, 43, 44], and especially automatic coarse spaces that  
 48 adapt to the variation in the properties of the media [22, 23, 42, 47, 15, 49, 48, 28,  
 49 27, 29, 36, 24]. In the latter, the coarse spaces are constructed from eigenfunctions  
 50 associated with small eigenvalues (low-frequency modes) of appropriated generalised  
 51 eigenvalue problems. This approach is backed up by rigorous mathematical theory  
 52 and has been numerically shown to be robust for general heterogeneous problems.  
 53 However, solving eigenvalue problems is expensive and extra implementation effort is  
 54 required as coarse spaces in DD methods are not naturally formulated as eigenfunc-  
 55 tions. Another approach is to use the deluxe scaling technique where local auxiliary  
 56 Dirichlet problems are solved to compute efficient averaging operators [33, 14, 52].  
 57 The approach yields robust DD methods, but extra implementation and computation  
 58 cost incur due to the auxiliary problems. In this paper, we formulate a *new balancing*  
 59 *DD by constraints (BDDC) preconditioner that requires no eigenvalue or auxiliary*  
 60 *problem and is very robust with the contrast of the coefficient.* The main motivation  
 61 behind this work is to achieve such goal while *maintaining the simplicity* of the BDDC  
 62 preconditioner.

63 The BDDC method was introduced by Dohrmann in 2003 [12]. It is an improved  
 64 version of the balancing DD (BDD) method by Mandel [38] and has a close connection  
 65 with the FETI-DP method [21, 20]. In fact, it can be shown that the eigenvalues  
 66 of the preconditioned operators associated with BDDC and FETI-DP are almost  
 67 identical [39, 34, 10]. The BDDC method is particularly well-suited for extreme scale  
 68 simulations, since it allows for a very aggressive coarsening, the computations at  
 69 different levels can be computed in parallel, the subdomain problems can be solved  
 70 inexactly [13, 35] by, e.g., one AMG cycle, and it can straightforwardly be extended  
 71 to multiple levels [51, 40]. All of these properties have been carefully exploited in  
 72 the series of articles [3, 4, 5, 6] where an extremely scalable implementation of these  
 73 algorithms has been proposed, leading to excellent weak scalability on nearly half a  
 74 million cores in its multilevel version.

75 Our new BDDC method is motivated from the fact that non-overlapping DD  
 76 methods, such as BDDC and FETI-DP, are robust with the variation and contrast  
 77 of the coefficient if it is constant (or varies mildly) in each subdomain [31, 30, 50].  
 78 This implies that in order to have robustness for BDDC methods one could use a  
 79 physics-based partition obtained by aggregating elements of the same coefficient value.  
 80 However, using this type of partition is impractical as the number of the subdomains  
 81 might be too large and can lead to a poor load balancing among subdomains and  
 82 large interfaces. In order to solve this dilemma, we propose to use a well-balanced  
 83 partition, e.g., one obtained from METIS [26] an automatic graph partitioner, to  
 84 distribute the work load among processors. Then, we consider a sub-partition of sub-  
 85 domains based on the physical coefficients, leading to a physic-based (PB) partition.  
 86 Continuity constraints among subdomains will be defined through the definition of  
 87 objects based on the PB partition. Consequently, the interface objects are adaptively  
 88 defined according to the variation of the coefficient. The resulting BDDC pre-  
 89 conditioner with constraints imposed on subfaces, subedges, and vertices will be called  
 90 PB-BDDC. These ideas can readily be applied to FETI-DP preconditioners.

91 We emphasise that the PB-BDDC method does not require to solve any eigenvalue  
 92 or auxiliary problems. Its formulation and implementation are very much the same

93 as for the standard BDDC method. The only difference is in identifying and defining  
 94 BDDC objects to impose constraints. In other words, *the simplicity of the standard*  
 95 *BDDC method is maintained.*

96 For multi-material problems, e.g., problems with isolated channels or inclusions,  
 97 it is possible to require the physical coefficient in each PB-subdomain to be constant.  
 98 In this situation, we are able to prove that *the new BDDC method is scalable and its*  
 99 *convergence is independent of the contrast of the coefficient.*

100 For heterogeneous problems with a wide spectrum of values in a small spatial  
 101 scale this restriction is too strong and might result in too many coarse objects (large  
 102 coarse problem). As a result, we also propose a relaxed definition of the PB partition  
 103 where we only require that the maximal contrast of the physical coefficient in each  
 104 PB-subdomain is smaller than a predefined threshold. The threshold can be chosen  
 105 so that the condition number is reasonably small while the size of the coarse problem  
 106 is not too large. We empirically show that this relaxed version of PB-BDDC, called  
 107 rPB-BDDC, is robust and efficient for different difficult distributions of the coefficient.

108 The rest of the paper is organised as follows. In [section 2](#), we introduce the model  
 109 problem, the domain partitions and the BDDC object classification. In [section 3](#), we  
 110 present the formulation of the (r)PB-BDDC methods as well as their key ingredients,  
 111 namely coarse degrees of freedom (coarse DOFs), weighting and harmonic extension  
 112 operators. The convergence analysis is also provided in this section. In [section 4](#),  
 113 we provide an extensive set of numerical experiments to demonstrate the robustness  
 114 and efficiency of the (r)PB-BDDC methods. We finally draw some conclusions in  
 115 [section 5](#).

116 **2. Problem setting.** Let  $\Omega \subset \mathbb{R}^d$ , with  $d$  being the space dimension, be a  
 117 bounded polyhedral domain. For a model problem, we study the Poisson's equa-  
 118 tion with non-constant diffusion and homogeneous Dirichlet conditions (the non-  
 119 homogeneous case only involves an obvious modification of the right-hand side). Thus,  
 120 the problem at hand is: find  $u \in H_0^1(\Omega)$  such that  $-\alpha \Delta u = f$  in  $H^{-1}(\Omega)$  sense, with  
 121  $f \in H^{-1}(\Omega)$  and  $\alpha \in L^\infty(\Omega)$  strictly positive. The weak form of the problem reads  
 122 as: find  $u^* \in H_0^1(\Omega)$  such that

$$123 \quad (1) \quad \int_{\Omega} \alpha \nabla u^* \cdot \nabla v \, dx = \int_{\Omega} f v \, dx, \quad \text{for any } v \in H_0^1(\Omega).$$

124 Let  $\mathcal{T}$  be a shape-regular quasi-uniform mesh of  $\Omega$  with characteristic size  $h$ . It can  
 125 consist of tetrahedra or hexahedra for  $d = 3$ , or triangles or quadrilaterals for  $d = 2$ .  
 126 For simplicity of exposition, we assume that  $\alpha$  is constant on each element  $\tau \in \mathcal{T}$ .

127 **2.1. Domain partitions.** We first consider a partition  $\Theta$  of  $\Omega$  into non-overlapping  
 128 open subdomains. This partition must be driven by computational efficiency in dis-  
 129 tributed memory platforms, i.e., it should have a reduced interface size and lead to  
 130 a well-balanced distribution of work load among processors. In a parallel implemen-  
 131 tation, each subdomain in  $\Theta$  is generally assigned to a processor. We further assume  
 132 that every  $\mathcal{D} \in \Theta$  can be obtained by *aggregation of elements* in  $\mathcal{T}$  and is connected.  
 133 We denote by  $\Gamma(\Theta)$  the interface of the partition  $\Theta$ , i.e.,  $\Gamma(\Theta) \doteq (\cup_{\mathcal{D} \in \Theta} \partial \mathcal{D}) \setminus \partial \Omega$ .

134 We also consider a PB subdomain partition. This partition is used latter in the  
 135 new definition of coarse objects and in the analysis. It is, however, not used for work  
 136 distribution. Given a subdomain  $\mathcal{D} \in \Theta$ , we can further consider its partition  $\Theta_{\text{pb}}(\mathcal{D})$   
 137 into a set of “sub-subdomains” with constant  $\alpha$ . The minimal set is preferred for  
 138 efficiency (it will potentially lead to a smaller coarse space) but it is not a requirement  
 139 (see [Remark 5](#)). Clearly, the resulting global PB partitions  $\Theta_{\text{pb}} \doteq \{\Theta_{\text{pb}}(\mathcal{D})\}_{\mathcal{D} \in \Theta}$

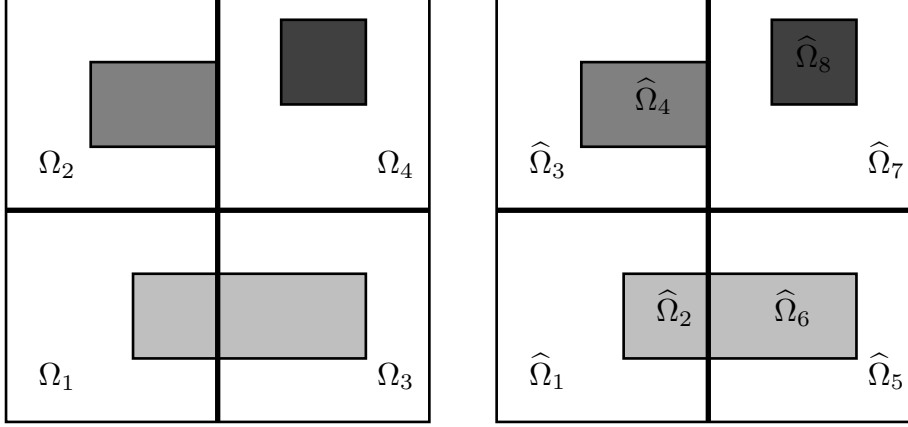


FIG. 1. An example of an original partition  $\Theta$  (left) and a physics-based partition  $\Theta_{\text{pb}}$  (right) of a square domain where different colors represent different values of  $\alpha$ . On the left, we have a  $\Theta = \{\Omega_1, \Omega_2, \Omega_3, \Omega_4\}$ . On the right, we show the corresponding PB-partition for every subdomains in  $\Theta$ :  $\Theta_{\text{pb}}(\Omega_1) = \{\hat{\Omega}_1, \hat{\Omega}_2\}$ ,  $\Theta_{\text{pb}}(\Omega_2) = \{\hat{\Omega}_3, \hat{\Omega}_4\}$ ,  $\Theta_{\text{pb}}(\Omega_3) = \{\hat{\Omega}_5, \hat{\Omega}_6\}$ , and  $\Theta_{\text{pb}}(\Omega_4) = \{\hat{\Omega}_7, \hat{\Omega}_8\}$ . The complete PB-partition is  $\Theta_{\text{pb}} = \{\hat{\Omega}_1, \dots, \hat{\Omega}_8\}$ . Further, we have  $\omega(\hat{\Omega}_1) = \omega(\hat{\Omega}_2) = \Omega_1$ ,  $\omega(\hat{\Omega}_3) = \omega(\hat{\Omega}_4) = \Omega_2$ ,  $\omega(\hat{\Omega}_5) = \omega(\hat{\Omega}_6) = \Omega_3$ ,  $\omega(\hat{\Omega}_7) = \omega(\hat{\Omega}_8) = \Omega_4$ .

140 is also a partition of  $\Omega$  (into PB subdomains). The interface of this partition is  
 141  $\Gamma(\Theta_{\text{pb}}) \doteq (\cup_{\hat{\mathcal{D}} \in \Theta_{\text{pb}}} \partial \hat{\mathcal{D}}) \setminus \partial \Omega$ . For a subdomain  $\mathcal{D} \in \Theta$  (analogously for  $\hat{\mathcal{D}} \in \Theta_{\text{pb}}$ ), we  
 142 denote by  $\mathcal{T}_{\mathcal{D}}$  the submesh of  $\mathcal{T}$  associated with  $\mathcal{D}$ ,  $\mathcal{T}_{\mathcal{D}} \doteq \{\tau \in \mathcal{T} : \tau \subset \mathcal{D}\} \subset \mathcal{T}$ . For  
 143 any  $\hat{\mathcal{D}} \in \Theta_{\text{pb}}$ , let  $\omega(\hat{\mathcal{D}})$  be the only subdomain in  $\Theta$  that contains  $\hat{\mathcal{D}}$ . In Figure 1, we  
 144 show an example of the original partition  $\Theta$  and the PB partition  $\Theta_{\text{pb}}$  for a simple  
 145 problem. The meaning of  $\Theta_{\text{pb}}(\mathcal{D})$  and  $\omega(\mathcal{D})$  is also illustrated.

146 **2.2. Finite element spaces.** Let us perform a discretization of (1) by a con-  
 147 tinuous finite element (FE) space  $\bar{\mathbb{V}}$  associated with the mesh  $\mathcal{T}$ . The discontinuous  
 148 Galerkin (DG) case will not be considered in this work, but we refer the reader to  
 149 [16] for more information.

150 For every subdomain  $\mathcal{D} \in \Theta$ , we consider a FE space  $\mathbb{V}_{\mathcal{D}}$  associated with the  
 151 local mesh  $\mathcal{T}_{\mathcal{D}}$ . Let  $H(\mathcal{D})$  be the characteristic length of the subdomain  $\mathcal{D}$  and  $h(\mathcal{D})$   
 152 be the characteristic length of the FE mesh  $\mathcal{T}_{\mathcal{D}}$ . We define the Cartesian product of  
 153 local FE spaces as  $\mathbb{V} = \prod_{\mathcal{D} \in \Theta} \mathbb{V}_{\mathcal{D}}$ . We note that functions in this space are allowed to  
 154 be discontinuous across the interface  $\Gamma(\Theta)$ . Clearly,  $\bar{\mathbb{V}} \subset \mathbb{V}$ .

155 For a subdomain  $\mathcal{D} \in \Theta$ , we also define the subdomain FE operator  $\mathcal{A}_{\mathcal{D}} : \mathbb{V}_{\mathcal{D}} \rightarrow$   
 156  $\mathbb{V}'_{\mathcal{D}}$  as  $\langle \mathcal{A}_{\mathcal{D}} u, v \rangle \doteq \int_{\mathcal{D}} \alpha \nabla u \cdot \nabla v \, dx$ , for all  $u, v \in \mathbb{V}_{\mathcal{D}}$ , and the sub-assembled operator  
 157  $\mathcal{A}^{\Theta} : \mathbb{V} \rightarrow \mathbb{V}'$  as  $\langle \mathcal{A}^{\Theta} u, v \rangle \doteq \sum_{\mathcal{D} \in \Theta} \langle \mathcal{A}_{\mathcal{D}} u, v \rangle$ , for all  $u, v \in \mathbb{V}$ .

158 A function  $u \in \mathbb{V}_{\mathcal{D}}$  is said to be discrete  $\alpha$ -harmonic in  $\mathcal{D}$  if

$$159 \quad \langle \mathcal{A}_{\mathcal{D}} u, v \rangle = 0, \quad \text{for any } v \in \mathbb{V}_{0, \mathcal{D}},$$

160 where  $\mathbb{V}_{0, \mathcal{D}} \doteq \{v \in \mathbb{V}_{\mathcal{D}} : v = 0 \text{ on } \partial \mathcal{D}\}$ . It should be noted that if  $u$  is discrete  
 161  $\alpha$ -harmonic in  $\mathcal{D}$  then it satisfies the energy minimising property, namely

$$162 \quad \langle \mathcal{A}_{\mathcal{D}} u, u \rangle \leq \langle \mathcal{A}_{\mathcal{D}} v, v \rangle, \quad \forall v \in \mathbb{V}_{\mathcal{D}}, v|_{\partial \mathcal{D}} = u|_{\partial \mathcal{D}}.$$

163 In addition, we consider the assembled operator  $\mathcal{A} : \bar{\mathbb{V}} \rightarrow \bar{\mathbb{V}}'$ , defined by  $\langle \mathcal{A} u, v \rangle =$   
 164  $\int_{\Omega} \alpha \nabla u \cdot \nabla v \, dx$ , for all  $u, v \in \bar{\mathbb{V}}$ . This operator is the Galerkin projection of  $\mathcal{A}^{\Theta}$  onto

165  $\bar{\mathbb{V}}$ . We want to compute a FE approximation  $u \in \bar{\mathbb{V}}$  of  $u^*$  in (1) such that

166 (2)  $\langle \mathcal{A}u, v \rangle = \langle f, v \rangle, \quad \text{for any } v \in \bar{\mathbb{V}}.$

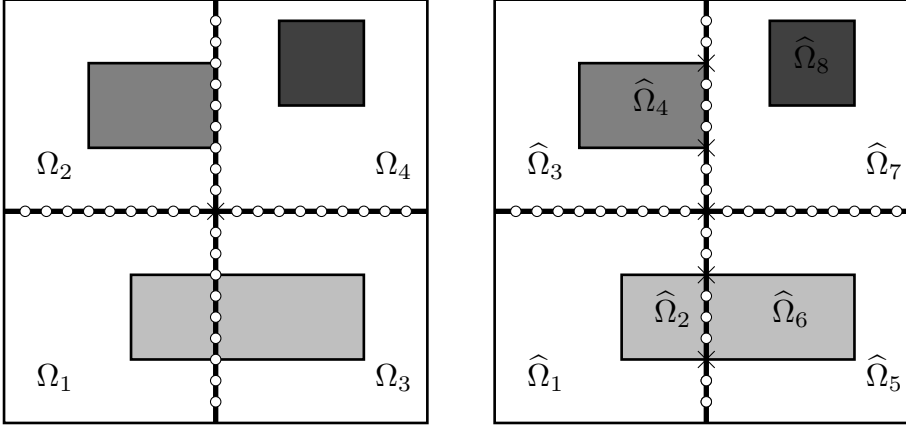


FIG. 2. An example of how FE nodes (on the interface of the original partition  $\Theta$  in Figure 1) are classified in the standard way (left) using  $\text{neigh}_{\Theta}$ , and in the physics-based way (right) using  $\text{neigh}_{\Theta_{\text{pb}}}$ . Corner nodes are marked with crosses while nodes in edges are marked with small circles. Using the standard classification, on the left, we obtain  $\Lambda(\Theta)$  with one corner and four edges. With the new classification, on the right, we have  $\Lambda_{\text{pb}}(\Theta)$  with five corners and six edges (eight edges if we only consider connected objects).

167 **2.3. Object classification.** This subsection concerns with objects on subdo-  
 168 main interfaces and their classification. It provides foundations for the definition of  
 169 coarse DOFs in BDDC methods later on.

170 Given a subdomain partition  $\Theta$ , and a point  $\xi \in \Gamma(\Theta)$ , let us denote by  $\text{neigh}_{\Theta}(\xi)$   
 171 the set of subdomains in  $\Theta$  that contain  $\xi$ . We can introduce the concept of objects  
 172 as a classification of points in  $\Gamma(\Theta)$ . A *geometrical object* is a maximal set  $\lambda$  of points  
 173 in  $\Gamma(\Theta)$  with identical subdomain set. We denote by  $\text{neigh}_{\Theta}(\lambda)$  the set of subdomains  
 174 in  $\Theta$  containing  $\lambda$ . It should be noted that the set of all geometrical objects, denoted  
 175 by  $\Lambda(\Theta)$ , is a partition of  $\Gamma(\Theta)$ .

176 *Remark 1.* Since the set of points in the interface is infinite, the previous classi-  
 177 fication of  $\Gamma(\Theta)$  into geometrical objects is performed in practice by the classification  
 178 of vertices, edges, and faces of elements in the mesh  $\mathcal{T}$  based on their subdomain set.

179 Denote by  $\text{ndof}(\lambda)$  the number of DOFs belonging to  $\lambda$ . We further consider the  
 180 following standard classification of geometrical objects. In the three-dimensional case,  
 181  $\lambda \in \Lambda(\Theta)$  is a *face* if  $|\text{neigh}_{\Theta}(\lambda)| = 2$  and  $\text{ndof}(\lambda) > 1$ , is an *edge* if  $|\text{neigh}_{\Theta}(\lambda)| > 2$  and  
 182  $\text{ndof}(\lambda) > 1$ , and is a *corner* if  $\text{ndof}(\lambda) = 1$ . In the two-dimensional case,  $\lambda \in \Lambda(\Theta)$   
 183 is an *edge* if  $|\text{neigh}_{\Theta}(\lambda)| = 2$  and  $\text{ndof}(\lambda) > 1$ , and is a *corner* if  $\text{ndof}(\lambda) = 1$ . In the  
 184 literature, e.g. [31, 50], corners are also referred to as vertices. Analogous definitions  
 185 are also used frequently for FETI-DP methods (see [50]). In Figure 2 (left), an  
 186 illustration of this classification is shown for a simple example.

187 In the next step, we define PB objects, which is the main ingredient of the PB-  
 188 BDDC methods proposed herein. We consider the set of objects  $\Lambda_{\text{pb}}(\Theta)$  obtained  
 189 by applying the previous classification of  $\Gamma(\Theta)$  into corners/edges/faces but with  
 190  $\text{neigh}_{\Theta}(\cdot)$  replaced by  $\text{neigh}_{\Theta_{\text{pb}}}(\cdot)$ . In other words, we use sets of subdomains in

191  $\Theta_{\text{pb}}$  to classify geometrical objects on  $\Gamma(\Theta)$ . **Figure 2** (right) shows objects in  $\Lambda_{\text{pb}}(\Theta)$   
 192 for a simple example.

193 **LEMMA 2.**  $\Lambda_{\text{pb}}(\Theta)$  is a refinement of  $\Lambda(\Theta)$ .

194 *Proof.* The statement holds if for every object  $\lambda_{\text{pb}} \in \Lambda_{\text{pb}}(\Theta)$  there exists one and  
 195 only one object  $\lambda \in \Lambda(\Theta)$  containing it. Since all points in  $\lambda_{\text{pb}}$  belong to the same set  
 196 of PB subdomains,  $\text{neigh}_{\Theta_{\text{pb}}}(\lambda)$ , they are in the same set of subdomains in  $\Theta$ , namely  
 197  $\{\omega(\hat{\mathcal{D}})\}_{\hat{\mathcal{D}} \in \text{neigh}_{\Theta_{\text{pb}}}(\lambda)}$ . As a result, all these points belong to the same object in  $\Lambda(\Theta)$ .  $\square$

198 **Remark 3.** In some cases, the DOF-based classification into corners, edges, and  
 199 faces might need some modification in order to ensure well-posedness of the BDDC  
 200 method with corner constraints only. This usually involves the use of a kernel detection  
 201 mechanism (see, e.g, [46]). A new approach based on perturbations has recently been  
 202 proposed in [8, 7], where the method is well-posed in all cases.

203 **Remark 4.** The PB aggregation (classification) of the interface  $\Gamma(\Theta)$  into  $\Lambda_{\text{pb}}(\Theta)$   
 204 can be relaxed. As it is currently stated, the PB partition is unique and have the min-  
 205 imal number of PB subdomains. However, it might introduces disconnected objects.  
 206 For example, the edge between  $\hat{\Omega}_3$  and  $\hat{\Omega}_7$  in **Figure 2** (right) is disconnected. Alter-  
 207 natively, one can require that objects must be connected. This leads to two connected  
 208 edges between  $\hat{\Omega}_3$  and  $\hat{\Omega}_7$ . We adopt this practice for the numerical experiments in  
 209 **section 4**. However, it should be noted that the use of disconnected objects leads to  
 210 a smaller coarse space and can be beneficial in some cases.

211 **Remark 5.** In practical implementations, one only needs the set of PB geometrical  
 212 objects  $\Lambda_{\text{pb}}(\Theta)$  to define the PB-BDDC preconditioner. When using the approach  
 213 with only connected objects (see **Remark 4**), one does not need to explicitly define  
 214 the PB partition  $\Theta_{\text{pb}}$ . Only a partition of objects in  $\Lambda(\Theta)$  (see **Figure 2** (left)) into PB  
 215 objects (see **Figure 2** (right)) based on the physical coefficients is required. Therefore,  
 216 only a  $(d - 1)$ -dimensional PB partition (of the interface  $\Gamma(\Theta)$ ) is needed. This is  
 217 what we have actually implemented for our numerical experiments in **section 4**. We  
 218 only use the PB partition  $\Theta_{\text{pb}}$  in the analysis in **subsection 3.4**. In any case, the PB  
 219 partition can easily be implemented if necessary.

220 **3. Physics-based BDDC preconditioning.** In this section, we present our  
 221 new PB-BDDC method. The basic idea behind BDDC methods is first to define a  
 222 sub-assembled operator (no assembling among subdomains), and the global space of  
 223 functions that are fully independent (“discontinuous”) among subdomains. Secondly,  
 224 we have to define the under-assembled space (the BDDC space) of functions for which  
 225 continuity among subdomains is enforced only on a set of coarse DOFs. In order to  
 226 be robust for heterogeneous problems, the PB-BDDC method utilises new definitions  
 227 of the BDDC space (i.e., new coarse DOF continuity among subdomains) and a new  
 228 weighting operator.

229 **3.1. Coarse degrees of freedom.** Similarly to other BDDC methods, in the  
 230 PB-BDDC method, some (or all) of the objects in  $\Lambda_{\text{pb}}(\Theta)$  are associated with a  
 231 coarse DOF. We denote this set of objects by  $\Lambda_O$  and call it the set of coarse objects.  
 232 Obviously,  $\Lambda_O \subset \Lambda_{\text{pb}}(\Theta)$ . Typical choices of  $\Lambda_O$  are  $\Lambda_O \doteq \Lambda_C$ , when only corners  
 233 are considered,  $\Lambda_O \doteq \Lambda_C \cup \Lambda_E$ , when corners and edges are considered, or  $\Lambda_O \doteq$   
 234  $\Lambda_{\text{pb}}(\Theta)$ , when corners, edges, and faces are considered. These choices lead to three  
 235 variants of the PB-BDDC method, referred to as PB-BDDC(c), PB-BDDC(ce) and  
 236 PB-BDDC(cef), respectively. **Figure 2** (right) actually shows the coarse objects of  
 237 PB-BDDC(ce) for a simple 2D problem.

238 Given an object  $\lambda \in \Lambda_O$ , we define its coarse DOF as the mean value on  $\lambda$ . The  
 239 rigorous definition is as follows. Assume  $\lambda \in \Lambda_O$  is associated with a subdomain  
 240  $\mathcal{D} \in \Theta$ . We define the coarse DOF  $c_\lambda^{\mathcal{D}}$  corresponding to  $\lambda$  as

$$241 \quad (3) \quad c_\lambda^{\mathcal{D}}(u_{\mathcal{D}}) \doteq \frac{\int_\lambda u_{\mathcal{D}} ds}{\int_\lambda 1 ds}, \quad \text{for } u_{\mathcal{D}} \in \mathbb{V}_{\mathcal{D}}.$$

242 Clearly,  $c_\lambda^{\mathcal{D}}$  is a functional in  $\mathbb{V}'_{\mathcal{D}}$ . When  $\lambda$  is a corner,  $c_\lambda^{\mathcal{D}}$  is simply the value at that  
 243 corner. Once we have defined the coarse DOFs, we can define the BDDC space as  
 244 follows

$$245 \quad (4) \quad \tilde{\mathbb{V}} \doteq \{v \in \mathbb{V} : c_\lambda^{\mathcal{D}}(v) = c_\lambda^{\mathcal{D}'}(v), \forall \lambda \in \Lambda_O, \forall \mathcal{D}, \mathcal{D}' \in \text{neigh}_\Theta(\lambda)\},$$

246 i.e., the subspace of functions in  $\mathbb{V}$  that are continuous ‘‘at’’ coarse DOFs. Clearly,  
 247  $\tilde{\mathbb{V}} \subset \tilde{\mathbb{V}} \subset \mathbb{V}$ .

248 For BDDC methods, solving the coarse problem is usually the bottleneck (cf.  
 249 [2, 3, 4, 8]). Therefore, it is of great interest to find a minimal set of coarse objects  
 250 (the number of the coarse objects is the number of the coarse DOFs and also is the  
 251 size of the coarse problem), so that BDDC methods can achieve their potential of  
 252 fast convergence and perfect weak scalability. According to [31, 50], in the case where  
 253 the physical coefficient in each subdomain is constant, the set of coarse objects only  
 254 need to guarantee the existence of the so-called *acceptable paths*. We need a similar  
 255 concept here for the PB-BDDC method.

256 The definition below is modelled after [50, Definition 6.26], [31] and [32].

257 **DEFINITION 6** (Acceptable path). *Let  $\Theta_{\text{pb}}^\partial$  be the set of PB subdomains  $\hat{\mathcal{D}} \in \Theta_{\text{pb}}$*   
 258 *touching the interface  $\Gamma(\Theta)$ , i.e.,  $\partial\hat{\mathcal{D}} \cap \Gamma(\Theta) \neq \emptyset$ . For two subdomains  $\hat{\mathcal{D}}_a, \hat{\mathcal{D}}_b \in \Theta_{\text{pb}}^\partial$*   
 259 *that share an edge  $\lambda$  but no face in  $\Lambda_{\text{pb}}(\Theta)$  or share a corner  $\lambda$  but no edge in  $\Lambda_{\text{pb}}(\Theta)$ ,*  
 260 *an acceptable path is a sequence  $\{\hat{\mathcal{D}}_a = \hat{\mathcal{D}}_1, \hat{\mathcal{D}}_2, \dots, \hat{\mathcal{D}}_n = \hat{\mathcal{D}}_b\}$  of PB subdomains in*  
 261  *$\Theta_{\text{pb}}^\partial$ , which satisfy the following properties:*

- 262 *i) they all share the common object  $\lambda \in \Lambda_{\text{pb}}(\Theta)$*
- 263 *ii) subdomains  $\hat{\mathcal{D}}_k$  and  $\hat{\mathcal{D}}_{k+1}$ ,  $k = 1, \dots, \hat{n} - 1$ , must share, apart from  $\lambda$ , an object*  
 264 *in  $\Lambda_O$  and the type of the shared object (face, edge or corner) must be the same*  
 265 *for the whole sequence*
- 266 *iii) their (constant) coefficients satisfy*

$$267 \quad \text{TOL } \alpha_k \geq R(k, \lambda) \min(\alpha_a, \alpha_b), \quad 1 \leq k \leq n$$

268 *where TOL is some predefined tolerance and  $R(k, \lambda) = 1$  if  $\lambda$  is an edge and*  
 269  *$R(k, \lambda) = h(\hat{\mathcal{D}}_k)/H(\hat{\mathcal{D}}_k)$  if  $\lambda$  is a corner.*

270 **Assumption 7.** We assume that the set of BDDC objects  $\Lambda_O$  satisfies the following  
 271 properties:

- 272 1. In the three dimensional case, for each face on  $\Gamma(\Theta)$ , there is at least one edge  
 273 that is part of its boundary and belongs to  $\Lambda_O$ .
- 274 2. For all pairs of subdomains  $\hat{\mathcal{D}}_a, \hat{\mathcal{D}}_b \in \Theta_{\text{pb}}^\partial$ , which have an edge but not a face  
 275 in  $\Lambda_{\text{pb}}(\Theta)$  in common, or a corner but not an edge in  $\Lambda_{\text{pb}}(\Theta)$  in common,  
 276 there exists an acceptable path for a predefined tolerance TOL.

277 **Remark 8.** In **Definition 6**, if the shared object  $\lambda$  belongs to the set of BDDC  
 278 objects  $\Lambda_O$ , then there exists a trivial acceptable path  $\{\hat{\mathcal{D}}_a, \hat{\mathcal{D}}_b\}$  with TOL = 1 and  
 279  $n = 2$ . Thus, BDDC(ce) and BDDC(cef) always satisfy **Assumption 7** for TOL = 1.

280 **3.2. Injection operators.** Let us define the projection  $\mathcal{Q} : \mathbb{V} \rightarrow \bar{\mathbb{V}}$  as some  
 281 weighted average of interface values together with an  $\alpha$ -harmonic extension to sub-  
 282 domain interiors (see, e.g., [39]). We define these ingredients as follows.

283 For  $u \in \mathbb{V}$  and  $\xi \in \Gamma(\Theta)$ , the weighting operator is defined as

$$284 \quad (5) \quad \mathcal{W}u(\xi) \doteq \sum_{\mathcal{D} \in \text{neigh}_{\Theta}(\xi)} \delta_{\mathcal{D}}^{\dagger}(\xi) u_{\mathcal{D}}(\xi), \quad \text{with} \quad \delta_{\mathcal{D}}^{\dagger}(\xi) \doteq \frac{\sum_{\tau \in \mathcal{T}_{\mathcal{D}}, \tau \ni \xi} \alpha_{\tau} |\tau|}{\sum_{\tau \in \mathcal{T}, \tau \ni \xi} \alpha_{\tau} |\tau|},$$

285 where  $|\tau|$  denotes the volume (area if in 2D) of the element  $\tau$ .

286 The  $\alpha$ -harmonic extension operator  $\mathcal{E}$  taking data on the interface  $\Gamma(\Theta)$  and  $\alpha$ -  
 287 harmonically extending it to each subdomain  $\mathcal{D} \in \Theta$  is formally defined as

$$288 \quad \mathcal{E}u \doteq (1 - \mathcal{A}_0^{-1} \mathcal{A})u,$$

289 where  $\mathcal{A}_0$  is the Galerkin projection of  $\mathcal{A}$  onto the bubble space  $\mathbb{V}_0 \doteq \{v \in \mathbb{V} : v =$   
 290  $0 \text{ on } \Gamma(\Theta)\}$ .

291 We finally define  $\mathcal{Q} = \mathcal{E}\mathcal{W}$ .

292 **3.3. PB-BDDC preconditioner.** In this subsection, we present the PB-BDDC  
 293 preconditioner, and describe its set-up and formulation. The PB-BDDC precondi-  
 294 tioner is a BDDC preconditioner in which the set of coarse DOFs enforce continuity  
 295 on a set of PB coarse objects, thus modifying the BDDC space being used. Once one  
 296 has defined the set of PB coarse objects  $\Lambda_{\mathcal{O}}$ , the rest of ingredients of the PB-BDDC  
 297 preconditioner are identical to the ones of a standard BDDC preconditioner. In any  
 298 case, the definition of the weighting operator introduced in (5) is new.

299 The BDDC preconditioner is a Schwarz-type preconditioner that combines interior  
 300 corrections with corrections in the BDDC space (see, e.g., [9, 50]). In case of the PB-  
 301 BDDC preconditioner, the BDDC correction is expressed as  $\mathcal{Q}(\tilde{\mathcal{A}}^{\Theta})^{-1} \mathcal{Q}^T$ , where  $\tilde{\mathcal{A}}^{\Theta}$  is  
 302 the Galerkin projection of  $\mathcal{A}^{\Theta}$  onto  $\bar{\mathbb{V}}$ . More specifically, the PB-BDDC preconditioner  
 303 reads as follows:

$$304 \quad \mathcal{B} = \mathcal{A}_0^{-1} + \mathcal{Q}(\tilde{\mathcal{A}}^{\Theta})^{-1} \mathcal{Q}^T.$$

305 Apart from the task of identifying and defining coarse objects, the implementation  
 306 of the PB-BDDC method is identical to that of the standard BDDC method. We  
 307 refer the interested reader to [12, 13, 40, 9] for more details on the formulation of  
 308 BDDC methods and to [2, 4, 6] for an efficient implementation of BDDC methods on  
 309 distributed memory machines, which requires much further elaboration.

310 **3.4. Condition number estimates.** In order to prove condition number esti-  
 311 mates for the PB-BDDC preconditioner, we first need to introduce  $\hat{\mathcal{B}}$ , an auxiliary  
 312 BDDC preconditioner. The definition of this preconditioner follows verbatim that  
 313 of the PB-BDDC preconditioner above but the PB subdomain partition  $\Theta_{\text{pb}}$  is used  
 314 instead of  $\Theta$ .

315 Given the FE mesh  $\mathcal{T}$ , the FE space type, and the subdomain partition  $\Theta_{\text{pb}}$ , one  
 316 can similarly build the FE spaces and operators as in subsection 2.2, leading to the  
 317 sub-assembled space  $\mathbb{V}^{\text{pb}}$  and operator  $\mathcal{A}^{\Theta_{\text{pb}}}$ . Further, we can define the injection  
 318 operator  $\hat{\mathcal{Q}}$  using the definitions in subsection 3.2 with  $\Theta$  is replaced by  $\Theta_{\text{pb}}$  for the  
 319 weighting  $\hat{\mathcal{W}}$  and harmonic extension  $\hat{\mathcal{E}}$  operators.

320 **LEMMA 9.** *For any PB subdomain  $\hat{\mathcal{D}} \in \Theta_{\text{pb}}$ , the function  $\delta_{\hat{\mathcal{D}}}^{\dagger}(\cdot)$  is constant on*  
 321 *each PB object  $\lambda$  associated with it, i.e.,*

$$322 \quad (6) \quad \delta_{\hat{\mathcal{D}}}^{\dagger}(\xi) = \delta_{\hat{\mathcal{D}}}^{\dagger}(\xi'), \quad \forall \xi, \xi' \in \lambda.$$

323 In addition, the following important inequality, cf. [50, 6.19], holds

$$324 \quad (7) \quad \alpha_{\widehat{\mathcal{D}}_a} \left( \delta_{\widehat{\mathcal{D}}_b}^\dagger(\xi) \right)^2 \leq C_{\delta^\dagger} \min \left( \alpha_{\widehat{\mathcal{D}}_a}, \alpha_{\widehat{\mathcal{D}}_b} \right), \quad \forall \widehat{\mathcal{D}}_a, \widehat{\mathcal{D}}_b \in \text{neigh}_{\Theta_{\text{pb}}}(\xi),$$

325 where  $C_{\delta^\dagger} \lesssim \max \left( 1, \frac{N_{\max}-1}{4} \right)$  with  $N_{\max}$  is the maximal number of elements in  $\mathcal{T}$   
326 sharing at least one point.

327 *Proof.* The identity (6) follows from (5), the fact that  $\alpha$  is constant in each sub-  
328 domain in  $\Theta_{\text{pb}}$  and  $\text{neigh}_{\Theta_{\text{pb}}}(\xi) = \text{neigh}_{\Theta_{\text{pb}}}(\xi') = \text{neigh}_{\Theta_{\text{pb}}}(\lambda)$ .

329 Now we need to verify (7). Since  $\alpha$  is constant in each PB subdomain, we can  
330 rewrite and bound  $\delta_{\widehat{\mathcal{D}}}^\dagger(\xi)$  as follows

$$331 \quad (8) \quad \delta_{\widehat{\mathcal{D}}_b}^\dagger(\xi) = \frac{\alpha_{\widehat{\mathcal{D}}_b} A_{\widehat{\mathcal{D}}_b}}{\sum_{\widehat{\mathcal{D}} \in \text{neigh}_{\text{pb}}(\xi)} \alpha_{\widehat{\mathcal{D}}} A_{\widehat{\mathcal{D}}}} < \frac{\alpha_{\widehat{\mathcal{D}}_b} A_{\widehat{\mathcal{D}}_b}}{\alpha_{\widehat{\mathcal{D}}_a} A_{\widehat{\mathcal{D}}_a} + \alpha_{\widehat{\mathcal{D}}_b} A_{\widehat{\mathcal{D}}_b}},$$

332 where  $A_{\widehat{\mathcal{D}}} > 0$  denotes the volume (area) of the patch of elements in  $\widehat{\mathcal{D}}$  containing  $\xi$ .

333 Clearly,  $\delta_{\widehat{\mathcal{D}}}^\dagger(\xi) \leq 1$ . Therefore,  $\alpha_{\widehat{\mathcal{D}}_a} (\delta_{\widehat{\mathcal{D}}_b}^\dagger(\xi))^2 \leq \alpha_{\widehat{\mathcal{D}}_a}$ . Now we need to prove that

$$334 \quad (9) \quad \alpha_{\widehat{\mathcal{D}}_a} \left( \delta_{\widehat{\mathcal{D}}_b}^\dagger(\xi) \right)^2 \leq C_{\delta^\dagger} \alpha_{\widehat{\mathcal{D}}_b}.$$

335 Using (8), it is sufficient to show

$$336 \quad (10) \quad \alpha_{\widehat{\mathcal{D}}_a} \alpha_{\widehat{\mathcal{D}}_b} A_{\widehat{\mathcal{D}}_b}^2 \leq C_{\delta^\dagger} (\alpha_{\widehat{\mathcal{D}}_a} A_{\widehat{\mathcal{D}}_a} + \alpha_{\widehat{\mathcal{D}}_b} A_{\widehat{\mathcal{D}}_b})^2.$$

337 Since the mesh  $\mathcal{T}$  is quasi-uniform, elements sharing at least a point have roughly the  
338 same volume (area). Consequently,  $A_{\widehat{\mathcal{D}}_b} \lesssim (N_{\max} - 1) A_{\widehat{\mathcal{D}}_a}$  (the worst case scenario is

339 when  $\widehat{\mathcal{D}}_b$  has  $N_{\max} - 1$  elements and  $\widehat{\mathcal{D}}_a$  has 1 element). Using this, we have

$$340 \quad \alpha_{\widehat{\mathcal{D}}_a} \alpha_{\widehat{\mathcal{D}}_b} A_{\widehat{\mathcal{D}}_b}^2 \lesssim (N_{\max} - 1) \alpha_{\widehat{\mathcal{D}}_a} \alpha_{\widehat{\mathcal{D}}_b} A_{\widehat{\mathcal{D}}_a} A_{\widehat{\mathcal{D}}_b} \leq \frac{N_{\max} - 1}{4} (\alpha_{\widehat{\mathcal{D}}_a} A_{\widehat{\mathcal{D}}_a} + \alpha_{\widehat{\mathcal{D}}_b} A_{\widehat{\mathcal{D}}_b})^2.$$

341 This implies (10) and we finish the proof.  $\square$

342 The definition of the set of coarse objects of  $\widehat{\mathcal{B}}$  requires further elaboration. The  
343 set of objects  $\Lambda(\Theta_{\text{pb}})$  obtained by applying the classification in subsection 2.3 for the  
344 PB subdomain partition  $\Theta_{\text{pb}}$  provides a classification of  $\Gamma(\Theta_{\text{pb}}) \supset \Gamma(\Theta)$ . We have the  
345 following relation between the PB objects  $\Lambda_{\text{pb}}(\Theta)$  and the (standard) objects of the  
346 PB partition  $\Lambda(\Theta_{\text{pb}})$ .

347 **LEMMA 10.** *All the objects in  $\Lambda_{\text{pb}}(\Theta)$  are also in  $\Lambda(\Theta_{\text{pb}})$ , i.e.,  $\Lambda_{\text{pb}}(\Theta) \subset \Lambda(\Theta_{\text{pb}})$ .*

348 *Proof.* Let us consider an object  $\lambda_{\text{pb}} \in \Lambda_{\text{pb}}(\Theta)$ . In both object partitions  $\Lambda_{\text{pb}}(\Theta)$   
349 and  $\Lambda(\Theta_{\text{pb}})$ , we are using the same criteria, i.e.,  $\text{neigh}_{\Theta_{\text{pb}}}(\cdot)$ , to classify points. The  
350 difference is that  $\Lambda_{\text{pb}}(\Theta)$  is the result of a classification of points in  $\Gamma(\Theta)$  whereas  
351  $\Lambda(\Theta_{\text{pb}})$  is obtained from a classification of points in  $\Gamma(\Theta_{\text{pb}})$ . Since  $\Gamma(\Theta) \subset \Gamma(\Theta_{\text{pb}})$ ,  
352 all points in  $\lambda_{\text{pb}}$  belong to the same object  $\lambda' \in \Lambda(\Theta_{\text{pb}})$ . Since  $\lambda_{\text{pb}}$  is on the in-  
353 terface  $\Gamma(\Theta)$ , there exist at least two subdomains  $\widehat{\mathcal{D}}, \widehat{\mathcal{D}}' \in \text{neigh}_{\Theta_{\text{pb}}}(\lambda_{\text{pb}})$  such that  
354  $\omega(\widehat{\mathcal{D}}) \neq \omega(\widehat{\mathcal{D}}')$ . Let us assume there is a point  $\xi \in \lambda'$  such that  $\xi \notin \lambda_{\text{pb}}$ . Then,  
355  $\xi \in \Gamma(\Theta_{\text{pb}}) \setminus \Gamma(\Theta)$ , i.e., it only belongs to one subdomain in  $\Theta$ . As a result,  $\omega(\widehat{\mathcal{D}})$  is  
356 the same for all  $\widehat{\mathcal{D}} \in \text{neigh}_{\Theta_{\text{pb}}}(\xi)$ . Thus, we have a contradiction, since  $\text{neigh}_{\Theta_{\text{pb}}}(\xi)$   
357 cannot be the same as  $\text{neigh}_{\Theta_{\text{pb}}}(\lambda_{\text{pb}})$ .  $\square$

358 With the theoretical support from [Lemma 10](#), we can define the set of coarse ob-  
 359 jects  $\widehat{\Lambda}_O$  of  $\widehat{\mathcal{B}}$  as a classification of  $\Gamma(\Theta_{\text{pb}})$  as follows. On  $\Gamma(\Theta)$ , we consider the  
 360 same set of objects  $\Lambda_O$  used in the PB-BDDC preconditioner, i.e.,  $\Lambda_C$ , or  $\Lambda_C \cup$   
 361  $\Lambda_E$ , or  $\Lambda_{\text{pb}}(\Theta)$ . For the rest of the interface  $\Gamma(\Theta_{\text{pb}}) \setminus \Gamma(\Theta)$ , we enforce *full conti-*  
 362 *nuity* among PB subdomains. It can be understood as treating all FE nodes on  
 363  $\Gamma(\Theta_{\text{pb}}) \setminus \Gamma(\Theta)$  as corners. Denote this set of objects by  $\widehat{\Lambda}^*$ , we have  $\widehat{\Lambda}_O = \Lambda_O \cup \widehat{\Lambda}^*$ .  
 364 [Figure 3](#) illustrates the partitions and coarse objects of  $\mathcal{B}$  and  $\widehat{\mathcal{B}}$  when  $\Lambda_O = \Lambda_C \cup \Lambda_E$ .  
 365

366 *Remark 11.* By construction, the BDDC space  $\widetilde{\mathbb{V}}^{\text{pb}}$  of the auxiliary BDDC pre-  
 367 conditioner  $\widehat{\mathcal{B}}$  is identical to the BDDC space  $\widetilde{\mathbb{V}}$ , defined in [\(4\)](#), of the PB-BDDC  
 368 preconditioner.

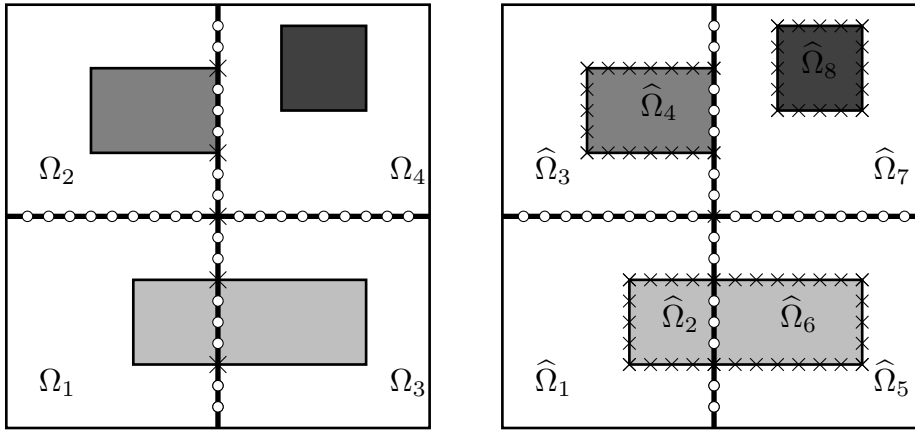


FIG. 3. Partitions and coarse objects of the PB-BDDC preconditioner  $\mathcal{B}$  (left) and the auxiliary BDDC preconditioner  $\widehat{\mathcal{B}}$  (right) when  $\Lambda_O = \Lambda_C \cup \Lambda_E$ : corner objects are labeled with crosses while nodes of other objects are labeled with circles.

369 **LEMMA 12.** *The condition number  $\kappa(\mathcal{B}\mathcal{A})$  of the PB-BDDC preconditioned oper-*  
 370 *ator is bounded by*

$$371 \quad (11) \quad \kappa(\mathcal{B}\mathcal{A}) \leq \max_{v \in \widetilde{\mathbb{V}}^{\text{pb}}} \frac{\langle \mathcal{A}^{\Theta_{\text{pb}}} \widehat{Q}v, \widehat{Q}v \rangle}{\langle \mathcal{A}^{\Theta_{\text{pb}}} v, v \rangle}.$$

372 *Proof.* According to [\[39, Theorem 15\]](#),  $\kappa(\mathcal{B}\mathcal{A})$  is bounded by

$$373 \quad (12) \quad \kappa(\mathcal{B}\mathcal{A}) \leq \max_{v \in \widetilde{\mathbb{V}}} \frac{\langle \mathcal{A}^{\Theta} Qv, Qv \rangle}{\langle \mathcal{A}^{\Theta} v, v \rangle}.$$

374 Now we only need to bound the right-hand-side in [\(12\)](#) by the one in [\(11\)](#).

On the one hand, using the fact that  $\widetilde{\mathbb{V}} = \widetilde{\mathbb{V}}^{\text{pb}}$ , we have  $\langle \mathcal{A}^{\Theta} v, v \rangle = \langle \mathcal{A}^{\Theta_{\text{pb}}} v, v \rangle$  for all  $v \in \widetilde{\mathbb{V}}$  because any  $v \in \widetilde{\mathbb{V}}$  is continuous in each subdomain of  $\Theta$ . On the other hand, let us prove that the weighting operator  $\widehat{\mathcal{W}}$  defined by [\(5\)](#) for  $\Theta_{\text{pb}}$  restricted to  $\mathbb{V}$  is identical to the weighting operator  $\mathcal{W}$  defined by [\(5\)](#) for  $\Theta$ . Let us consider a subdomain  $\mathcal{D} \in \Theta$  and its PB partition  $\Theta_{\text{pb}}(\mathcal{D})$ . We have

$$\delta_{\mathcal{D}}^{\dagger}(\xi) = \sum_{\widehat{\mathcal{D}} \in \Theta_{\text{pb}}(\mathcal{D}), \widehat{\mathcal{D}} \ni \xi} \delta_{\widehat{\mathcal{D}}}^{\dagger}(\xi),$$

375 by the definition in (5). For an arbitrary function  $v \in \mathbb{V} \subset \mathbb{V}^{\text{pb}}$ , we find that

$$\begin{aligned}
376 \quad \mathcal{W}v(\xi) &= \sum_{\mathcal{D} \in \text{neigh}_{\Theta}(\xi)} \delta_{\mathcal{D}}^{\dagger}(\xi) v_{\mathcal{D}}(\xi) = \sum_{\mathcal{D} \in \text{neigh}_{\Theta}(\xi)} \sum_{\hat{\mathcal{D}} \in \Theta_{\text{pb}}, \hat{\mathcal{D}} \ni \xi} \delta_{\hat{\mathcal{D}}}^{\dagger}(\xi) v_{\mathcal{D}}(\xi) \\
377 \quad &= \sum_{\hat{\mathcal{D}} \in \text{neigh}_{\Theta_{\text{pb}}}(\xi)} \delta_{\hat{\mathcal{D}}}^{\dagger}(\xi) v_{\hat{\mathcal{D}}}(\xi) = \widehat{\mathcal{W}}v(\xi). \\
378
\end{aligned}$$

379 Therefore,  $\widehat{\mathcal{Q}}v$  and  $\mathcal{Q}v$  are identical on  $\Gamma(\Theta)$  and  $\widehat{\mathcal{Q}}v$  is continuous across  $\Gamma(\Theta_{\text{pb}})$ . In  
380 addition,  $\mathcal{Q}v$  is discrete  $\alpha$ -harmonic in each  $\mathcal{D} \in \Theta$  and have minimal energy norm  
381 w.r.t  $\mathcal{A}^{\Theta}$ . As a consequence,

$$\begin{aligned}
382 \quad \langle \mathcal{A}^{\Theta} \mathcal{Q}v, \mathcal{Q}v \rangle &= \sum_{\mathcal{D} \in \Theta} \langle \mathcal{A}_{\mathcal{D}}^{\Theta} \mathcal{Q}v, \mathcal{Q}v \rangle \\
383 \quad &\leq \sum_{\mathcal{D} \in \Theta} \langle \mathcal{A}_{\mathcal{D}}^{\Theta} \widehat{\mathcal{Q}}v, \widehat{\mathcal{Q}}v \rangle = \sum_{\hat{\mathcal{D}} \in \Theta_{\text{pb}}} \langle \mathcal{A}_{\hat{\mathcal{D}}}^{\Theta_{\text{pb}}} \widehat{\mathcal{Q}}v, \widehat{\mathcal{Q}}v \rangle = \langle \mathcal{A}^{\Theta_{\text{pb}}} \widehat{\mathcal{Q}}v, \widehat{\mathcal{Q}}v \rangle. \\
384
\end{aligned}$$

385 This finishes the proof.  $\square$

386 We could stop here and derive the estimate for  $\kappa(\mathcal{BA})$  knowing that the condition  
387 number of the auxiliary BDDC preconditioned operator  $\widehat{\mathcal{B}}\mathcal{A}$  is estimated by an upper  
388 bound of the last quantity on the right of (12). However, we will go a bit further to  
389 obtain a stronger result.

390 LEMMA 13. Assume that  $\Lambda_O$  is such that Assumption 7 holds. Then we have the  
391 following inequality:

$$392 \quad (13) \quad \max_{v \in \widetilde{\mathbb{V}}^{\text{pb}}} \frac{\langle \mathcal{A}^{\Theta_{\text{pb}}} \widehat{\mathcal{Q}}v, \widehat{\mathcal{Q}}v \rangle}{\langle \mathcal{A}^{\Theta_{\text{pb}}} v, v \rangle} \leq C \max\{1, \text{TOL}\} \max_{\mathcal{D} \in \Theta_{\text{pb}}} \left( 1 + \log \left( \frac{H(\mathcal{D})}{h(\mathcal{D})} \right) \right)^2,$$

393 where the constant  $C$  is independent of the number of subdomains,  $H(\hat{\mathcal{D}})$ ,  $h(\hat{\mathcal{D}})$  and  
394 the physical coefficient  $\alpha$ .

395 *Proof.* By triangle inequality, we have

$$396 \quad (14) \quad \max_{v \in \widetilde{\mathbb{V}}^{\text{pb}}} \frac{\langle \mathcal{A}^{\Theta_{\text{pb}}} \widehat{\mathcal{Q}}v, \widehat{\mathcal{Q}}v \rangle}{\langle \mathcal{A}^{\Theta_{\text{pb}}} v, v \rangle} \leq 1 + \max_{v \in \widetilde{\mathbb{V}}^{\text{pb}}} \frac{\langle \mathcal{A}^{\Theta_{\text{pb}}} (\widehat{\mathcal{Q}}v - v), (\widehat{\mathcal{Q}}v - v) \rangle}{\langle \mathcal{A}^{\Theta_{\text{pb}}} v, v \rangle}.$$

397 Let  $w = \widehat{\mathcal{Q}}v - v$ . Given a FE function  $u \in \mathbb{V}_{\hat{\mathcal{D}}}$ , we denote by  $\theta_{\lambda}^{\hat{\mathcal{D}}}(u) \in \mathbb{V}_{\hat{\mathcal{D}}}$  the FE  
398 function that is discrete  $\alpha$ -harmonic in  $\hat{\mathcal{D}}$  and agrees with  $u$  at the FE nodes in the  
399 object  $\lambda$  and vanishes at all the other nodes on  $\partial\hat{\mathcal{D}}$ . Since  $\Lambda(\Theta_{\text{pb}})$  is a partition of  
400  $\Gamma(\Theta_{\text{pb}})$ , we can split  $w$  into object and subdomain contributions as follows:

$$401 \quad (15) \quad w = \sum_{\lambda \in \Lambda(\Theta_{\text{pb}})} \sum_{\hat{\mathcal{D}} \in \text{neigh}_{\Theta_{\text{pb}}}(\lambda)} \theta_{\lambda}^{\hat{\mathcal{D}}}(w).$$

402 By the construction of the set of object  $\widehat{\Lambda}_O = \Lambda_O \cup \widehat{\Lambda}^*$  and the definition of  $\widetilde{\mathbb{V}}^{\text{pb}}$ ,  $w$   
403 vanishes at all coarse objects in  $\widehat{\Lambda}^*$ , i.e, at all FE nodes in  $\Gamma(\Theta_{\text{pb}}) \setminus \Gamma(\Theta)$ . Consequently,  
404 (15) can be simplified as follows:

$$405 \quad (16) \quad w = \sum_{\lambda \in \Lambda_{\text{pb}}(\Theta)} \sum_{\hat{\mathcal{D}} \in \Theta_{\text{pb}}^{\theta}} \theta_{\lambda}^{\hat{\mathcal{D}}}(w).$$

406 When  $\Lambda_O$  satisfies [Assumption 7](#), the set of objects in  $\widehat{\Lambda}_O$  also fulfils [[50](#), Assump-  
 407 tion 6.27]. Consequently, using [Lemma 9](#), we can perform an analysis similar to that  
 408 in the proof [[50](#), Lemma 6.36] (see also [[31](#), Lemma 10]) to obtain

$$409 \quad \langle \mathcal{A}_{\widehat{\mathcal{D}}}^{\Theta_{\text{pb}}} \theta_{\lambda}^{\widehat{\mathcal{D}}}(w), \theta_{\lambda}^{\widehat{\mathcal{D}}}(w) \rangle$$

$$410 \quad \leq C \max\{1, \text{TOL}\} \left( 1 + \log \left( \frac{H(\widehat{\mathcal{D}})}{h(\widehat{\mathcal{D}})} \right) \right)^2 \sum_{\widehat{\mathcal{D}} \in \text{neigh}_{\Theta_{\text{pb}}}(\lambda)} \langle \mathcal{A}_{\widehat{\mathcal{D}}}^{\Theta_{\text{pb}}} v, v \rangle$$

411  
 412 for any  $\widehat{\mathcal{D}} \in \Theta_{\text{pb}}^{\partial}$  and  $\lambda \in \Lambda(\Theta_{\text{pb}})$ . Here the constant  $C$  is proportional to  $C_{\delta\uparrow}$  in  
 413 [Lemma 9](#), but is otherwise independent of  $H(\widehat{\mathcal{D}})$ ,  $h(\widehat{\mathcal{D}})$  and the physical coefficient  $\alpha$ .

414 Adding up the estimate for all subdomain  $\widehat{\mathcal{D}} \in \Theta_{\text{pb}}$ , we find that

$$415 \quad (17) \quad \langle \mathcal{A}^{\Theta_{\text{pb}}} w, w \rangle \leq C \max\{1, \text{TOL}\} \max_{\widehat{\mathcal{D}} \in \Theta_{\text{pb}}^{\partial}} \left( 1 + \log \left( \frac{H(\widehat{\mathcal{D}})}{h(\widehat{\mathcal{D}})} \right) \right)^2 \langle \mathcal{A}^{\Theta_{\text{pb}}} v, v \rangle.$$

416 This finishes the proof.  $\square$

417 Combining results in [Lemma 12](#) and [Lemma 13](#), we have the final bound for  
 418 the PB-BDDC preconditioner, which is both weakly scalable and independent of the  
 419 coefficient  $\alpha$ .

420 **THEOREM 14.** *The condition number of the PB-BDDC preconditioned operator*  
 421  *$\kappa(\mathcal{BA})$  is bounded by*

$$422 \quad \kappa(\mathcal{BA}) \leq C \max\{1, \text{TOL}\} \max_{\widehat{\mathcal{D}} \in \Theta_{\text{pb}}^{\partial}} \left( 1 + \log \left( \frac{H(\widehat{\mathcal{D}})}{h(\widehat{\mathcal{D}})} \right) \right)^2,$$

423 where the constant  $C$  is independent of the number of subdomains,  $H(\widehat{\mathcal{D}})$ ,  $h(\widehat{\mathcal{D}})$  and  
 424 the physical coefficient  $\alpha$ .

425 *Remark 15.* As seen in the [Lemma 13](#) and [Theorem 14](#), the condition number  
 426 associated with the PB-BDDC method depends only on the characteristic size and  
 427 mesh size of PB subdomains touching the original interface  $\Gamma(\Theta)$ . Further, the con-  
 428 vergence of the PB-BDDC is independent of variations of the coefficient. The main  
 429 target of this work is achieved.

430 **3.5. Relaxed physics-based BDDC.** The definition of the coarse objects for  
 431 the PB-BDDC preconditioner, based on the requirement that the coefficient has to  
 432 be constant in each PB subdomain, can result in a large coarse space. That is the  
 433 case for heterogeneous problems where the physical coefficient varies across a wide  
 434 spectrum of values in a small spatial scale.

435 In order to deal with a more general class of problems, we propose the relaxed PB-  
 436 BDDC preconditioner (rPB-BDDC) where we only require that the maximal contrast  
 437 in each PB subdomain is less than some predefined tolerance  $r$ . We consider a relaxed  
 438 PB partition  $\Theta^{\text{pb}}$  such that

$$439 \quad (18) \quad \max_{\tau, \tau' \subset \widehat{\mathcal{D}}} \frac{\alpha_{\tau}}{\alpha_{\tau'}} \leq r, \quad \text{for any } \widehat{\mathcal{D}} \in \Theta^{\text{pb}}.$$

440 Here the threshold  $r$  is equal or greater than 1. This way, we can control the size of  
 441 the coarse problem and the condition number bounds with the choice of  $r$ .

442 As the coefficient is no longer constant in each PB subdomain, we need to use  
 443 a weighted-constraint in the definition of coarse DOFs. More specifically, instead of  
 444 using (3), we use

$$445 \quad (19) \quad c_{\lambda}^{\mathcal{D}}(u) \doteq \frac{\int_{\lambda} \bar{\alpha} u ds}{\int_{\lambda} \bar{\alpha} 1 ds}, \quad \text{where } \bar{\alpha}(\xi) \doteq \max_{\tau \in \mathcal{T}, \tau \ni \xi} \alpha_{\tau}.$$

446

447 *Remark 16.* The larger  $r$  becomes the smaller the size of the coarse problem of the  
 448 rPB-BDDC preconditioner is and the larger its condition number grows to. When  
 449  $r = 1$  the rPB-BDDC preconditioner becomes the PB-BDDC preconditioner. By  
 450 tuning the threshold  $r$ , one can obtain a right balance between the time spent on  
 451 setting up the preconditioner (especially in forming the coarse space) and the time  
 452 spent on applying the preconditioner in a Krylov solver. The optimal threshold is of  
 453 course problem dependent. However, finding a good threshold is not tricky. This is  
 454 illustrated in section 4.

455 *Remark 17.* The rPB-BDDC preconditioner makes use of a threshold. This is sim-  
 456 ilar to the adaptive coarse space approach where only eigenfunctions associated with  
 457 eigenvalues below a predefined threshold are included in the coarse space. However,  
 458 the rPB-BDDC preconditioner does not involve any eigenvalue or auxiliary problems  
 459 and is far simpler and cheaper.

460 **4. Numerical experiments.** In this section, we test the robustness and effi-  
 461 ciency of the PB-BDDC and rPB-BDDC preconditioners for the system matrix asso-  
 462 ciated with (2) for different types of variation in the coefficient  $\alpha$ , which are similar  
 463 but generally harder than the ones in [42, 28, 36].

464 Due to the difficulty of heterogeneous problems, in PB-BDDC and rPB-BDDC  
 465 methods, we tend to use a large number of objects. Many of them are not corners. In  
 466 all tested cases, these objects are enough to make the local Neumann problems and  
 467 global coarse problem well-posed and we can optionally drop corner objects. No corner  
 468 detection mechanism (see, e.g, [46]) has been needed in any tested case. Alternatively,  
 469 one might want to consider the perturbed formulation introduced in [7, 8]. However,  
 470 this approach has not been extended to heterogeneous problems yet.

471 In all of the experiments, we consider the physical domain  $\Omega = (0, 1)^2$ . Unless  
 472 stated otherwise, we use the uniform triangular meshes of size  $h = 1/72$  and the  
 473 regular  $3 \times 3$  subdomain partition. In all cases, we report the dimension of the  
 474 coarse space, denoted by  $\dim$ , and the number of iterations required for the conjugate  
 475 gradient method to reduce the residual norm by a factor of  $10^6$ . We also provide the  
 476 condition number  $\kappa$  in most examples.

477 **4.1. Two channels.** In this test case, we consider two channels of high  $\alpha$  cutting  
 478 through vertical subdomain edges (see Figure 4). The coefficient in the channels  $\alpha_{\max}$   
 479 takes the values  $\{10^2, 10^4, 10^6, 10^8\}$ , while the coefficient in the rest of the domain  
 480 is equal to 1.

481 From Table 1, we can see that the condition number and the number of iter-  
 482 ations for the standard BDDC preconditioner (BDDC(ce)) definitely increase with  
 483  $\alpha_{\max}$ , whereas they remain practically constant for both variants of the PB-BDDC  
 484 preconditioners (PB-BDDC(ce) and PB-BDDC(e)). In other words, the convergence  
 485 of the PB-BDDC method is independent of the contrast and the PB-BDDC method is  
 486 perfectly robust for this test case. Figure 4 shows the coarse objects of PB-BDDC(ce)  
 487 on the interface of the partition.

TABLE 1  
Comparison of the iteration count and condition number in the two channels test case.

dim $\rightarrow$	BDDC(ce)		PB-BDDC(ce)		PB-BDDC(e)	
	16		64		36	
$\alpha_{\max}$	# it.	$\kappa$	# it.	$\kappa$	# it.	$\kappa$
$10^2$	21	2.12e3	10	5.47e0	13	1.20e1
$10^4$	28	2.87e5	10	5.31e0	14	1.21e1
$10^6$	44	2.89e7	10	5.31e0	15	1.21e1
$10^8$	64	3.88e9	10	5.31e0	15	1.21e1

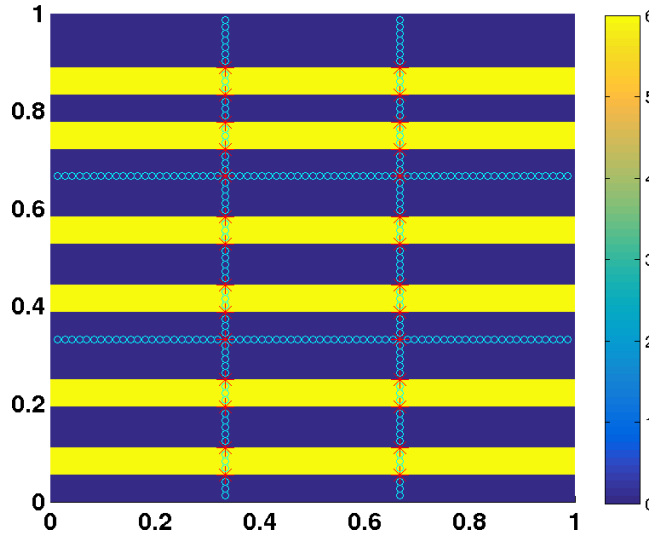


FIG. 4. Distribution of the coefficient in the two-channels test case when  $\alpha_{\max} = 10^6$ . The coarse objects of PB-BDDC(ce) are shown on the interface with corners labeled by stars and DOFs in edges labeled by circles.

488 **4.2. Channels and inclusions.** In this test case, we consider both channels  
 489 and inclusions of high coefficient. First, the three channels include all the elements  
 490 whose centroids are less than  $2 \cdot 10^{-2}$  from one of the following three lines:

$$\begin{aligned}
 491 \quad & L1 : x_1 - x_2 - 0.2 = 0, \\
 492 \quad & L2 : x_1 + x_2 - 0.7 = 0, \\
 493 \quad & L3 : x_1 - 0.7x_2 - 0.7 = 0.
 \end{aligned}$$

495 The coefficient  $\alpha_{\max}$  in these channels takes the values  $\{10^2, 10^4, 10^6, 10^8\}$ . Secondly,  
 496 the inclusions are defined as the regions of elements whose all vertices  $x$  satisfy

$$497 \quad \text{mod}(\text{floor}(10x_i), 2) = 1, \text{ for } i = 1, 2.$$

498 For an element  $\tau$  that belongs to one of the inclusions and is not in the channels, its  
 499 coefficient is defined as

$$500 \quad (20) \quad \alpha|_{\tau} = (\alpha_{\max}/10)^{1/5 * \text{floor}(0.5 * \text{floor}(10x_1(c_{\tau})) + 1)}, \quad \text{where } c_{\tau} \text{ is the centroid of } \tau.$$

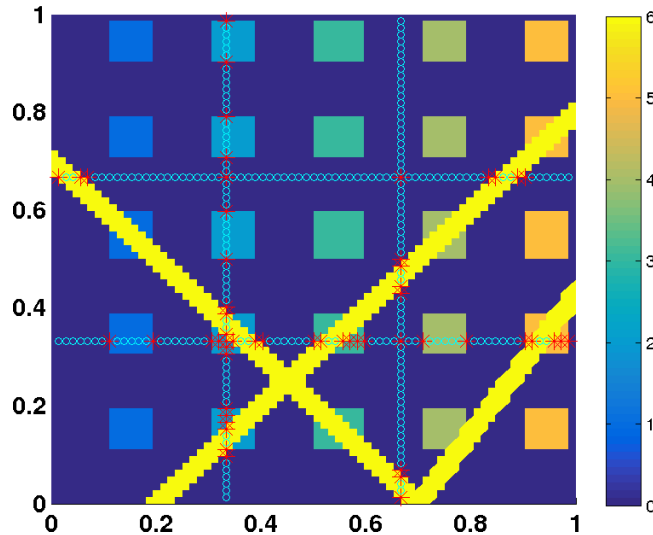


FIG. 5. Distribution of the coefficient for the channels and inclusions test case when  $\alpha_{\max} = 10^6$ . The coarse objects of PB-BDDC(ce) are shown on the interface with corners labeled by stars and DOFs in edges labeled by circles.

501 The coefficient in (20) is: a) constant in each inclusion b) increasing from left to right  
 502 c) increasing as  $\alpha_{\max}$  increases and d) always belongs to  $(1, \alpha_{\max})$ . For the rest of the  
 503 domain, we set  $\alpha = 1$ . The maximal contrast ratio in this experiment is  $10^8$ .

504 We can see from Table 2 that as  $\alpha_{\max}$  becomes larger the condition number and  
 505 the number of iterations associated with the standard BDDC(ce) method increases  
 506 significantly. In contrast, both variant of the PB-BDDC methods, PB-BDDC(ce) and  
 507 PB-BDDC(e), are perfectly robust with respect to the changes of the coefficient in  
 508 the channels and in the inclusions. Especially, PB-BDDC(e) maintains its robustness  
 509 with a reasonably small coarse space.

TABLE 2

Comparison of the iteration count and condition number in the channels and inclusions test case.

dim $\rightarrow$	BDDC(ce)		PB-BDDC(ce)		PB-BDDC(e)	
	16		89		39	
$\alpha_{\max}$	# it.	$\kappa$	# it.	$\kappa$	# it.	$\kappa$
$10^2$	23	1.48e3	13	1.01e1	14	5.71e1
$10^4$	45	8.33e4	13	8.93e0	15	8.08e1
$10^6$	82	6.02e6	13	8.79e0	15	8.15e1
$10^8$	97	5.30e8	13	8.76e0	15	8.15e1

510 **4.3. Complex channels.** In this test case, we demonstrate the importance of  
 511 having acceptable paths. We consider a distribution with multiple channels of high  
 512 coefficient  $\alpha_{\max}$  taking values in  $\{10^2, 10^4, 10^6, 10^8\}$  (see Figure 6 for the case when  
 513  $\alpha_{\max} = 10^6$ ).

514 From Table 3, we can see that PB-BDDC(ce) is perfectly robust. On the other  
 515 hand, the condition number and number of iterations of the PB-BDDC(e) precon-

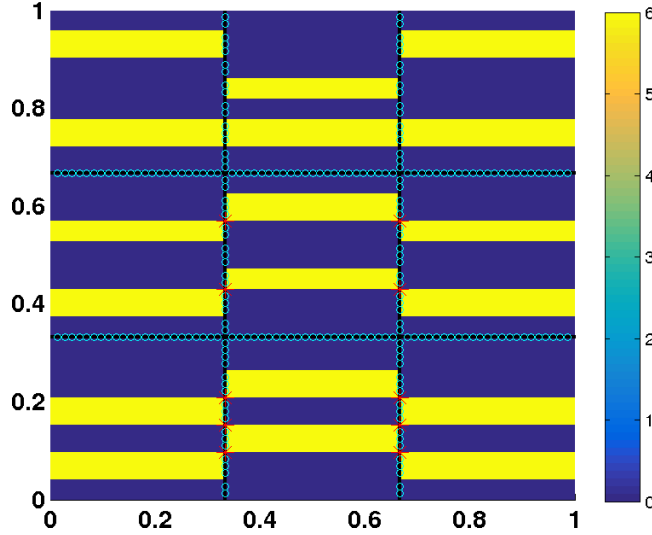


FIG. 6. Distribution of the coefficient in the complex channels test case. The coarse objects of PB-BDDC([c]e) are shown on the interface with corners labeled by stars and DOFs in edges labeled by circles. Only few corners are required to guarantee perfect robustness (to have acceptable paths).

516 ditioner increase significantly as  $\alpha_{\max}$  increases. The reason is that there are some  
 517 pairs of channels share a corner but not an edge. In PB-BDDC(e), none of these  
 518 corners are selected as a coarse objects. Consequently, there is no acceptable path  
 519 with TOL independent of the contrast between the associated paired of channels (PB  
 520 subdomains) and Assumption 7 does not hold. By including a small number of these  
 521 critical corners (represented by stars in Figure 6) in order to satisfy Assumption 7, the  
 522 resulting preconditioner, labeled PB-BDDC([c]e), is perfectly robust w.r.t changes in  
 523 the contrast of the coefficient (see Table 3).

TABLE 3  
 Comparison of the iteration count and condition number in the complex channels test case.

	BDDC(ce)	PB-BDDC(ce)	PB-BDDC(e)	PB-BDDC([c]e)
dim	16	84	46	56
$\alpha_{\max}$	# it. ( $\kappa$ )			
$10^2$	22 (2.99e3)	12 (6.09e0)	19 (1.25e3)	13 (1.21e1)
$10^4$	43 (3.82e5)	12 (5.94e0)	34 (1.62e5)	13 (1.27e1)
$10^6$	70 (3.83e7)	12 (5.94e0)	51 (1.63e7)	13 (1.27e1)
$10^8$	95 (6.45e9)	12 (5.94e0)	99 (1.63e9)	13 (1.27e1)

524 **4.4. Sinusoidal variation.** In this experiment, we consider a coefficient that  
 525 varies like a sinusoid. We use a finer uniform triangular mesh of size  $h = 1/144$ . For  
 526 an element  $\tau \in \mathcal{T}$ , the coefficient  $\alpha_\tau$  is defined by

$$527 \quad \log_{10}(\alpha_\tau) = \kappa \sin(w\pi(x_1(c_\tau) + x_2(c_\tau))) + \alpha_{\text{shift}},$$

528 where  $\kappa = 3$ ,  $w = 14$ , and  $c_\tau$  is the the centroid of  $\tau$ . We note that when  $\kappa$  and/or  
 529  $w$  become larger the problem is more difficult. The distribution when  $\alpha_{\text{shift}} = 0$  is

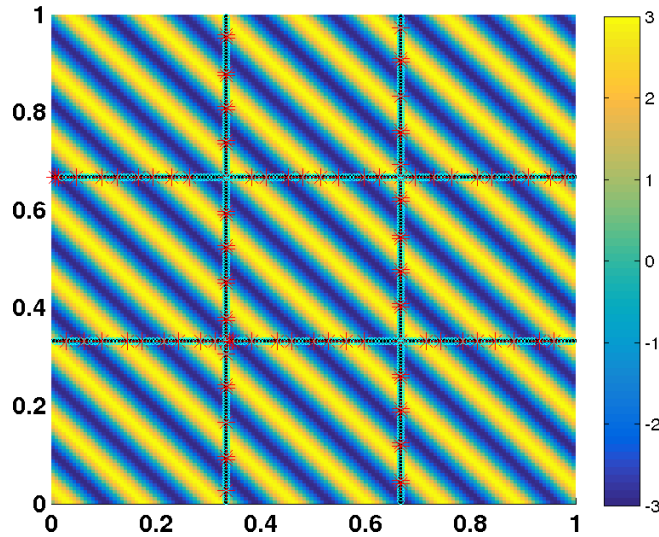


FIG. 7. Distribution of the coefficient mimicking sin function. The coarse objects of rPB-BDDC(ce) with  $r = 10^3$  are shown on the interface with corners labeled by stars and DOFs in edges labeled by circles.

530 shown in Figure 7. It is as if there are many channels going through subdomain edges  
 531 at the same time.

532 In this test case, the coefficient varies very rapidly. We test the standard BDDC  
 533 method and the rPB-BDDC method introduced in subsection 3.5, by allowing the  
 534 upper bound  $r$  for the maximal contrast in each PB subdomain to vary among  
 535  $\{10^1, 10^2, 10^3\}$ . Only iteration counts are reported as the condition number estimation  
 536 becomes too expensive for the mesh being used.

537 This is a difficult problem and the standard BDDC(ce) method requires almost  
 538 a hundred iterations to converge (see Table 4). The relaxed physics-based methods,  
 539 rPB-BDDC(ce) and rPB-BDDC(e), are able to significantly reduce the number of  
 540 iterations. That comes with the cost of solving larger coarse problems. However, by  
 541 using a suitable threshold  $r$ , we can obtain a decent preconditioner, e.g. rPB-BDDC(e)  
 542 with  $r = 10^3$ , which requires only 11 iterations using a reasonably small coarse space  
 543 of size 64. In addition, the rPB-BDDC method is also perfectly robust with shifting  
 544 in the value of the coefficient. The iteration count does not change when  $\alpha_{\text{shift}}$  takes  
 545 values in  $\{0, 6\}$ .

TABLE 4  
 Comparison of the iteration count in the continuous sin test case.

		BDDC(ce)	rPB-BDDC(ce)			rPB-BDDC(e)		
$r$			10	$10^2$	$10^3$	10	$10^2$	$10^3$
	dim	16	474	292	188	212	116	64
$\alpha_{\text{shift}} = 0$	# it.	92	7	10	11	10	12	11
$\alpha_{\text{shift}} = 6$	# it.	99	7	10	11	10	12	11

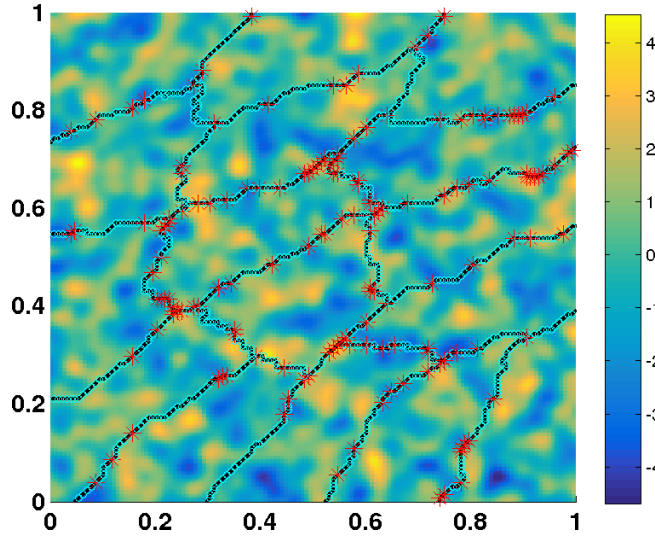


FIG. 8. *Distribution of the coefficient in the log-normal test case. The coarse objects of rPB-BDDC(ce) with  $r = 10^2$  are shown on the interface with corners labeled by stars and DOFs in edges labeled by circles.*

546 **4.5. Log-Normal.** In this test case, we test the performance of the rPB-BDDC  
 547 method for a log-normal distribution of the coefficient. This type of distribution is  
 548 particularly important for geoscience and petroleum engineering applications. We  
 549 consider  $\alpha_{\text{cont}}(x, w) = 10^{Z(x, w)}$ , where  $Z(x, w)$  is a Gaussian random field with zero  
 550 mean and Gaussian covariance

$$551 \quad C(x, y) = \sigma^2 \exp\left(-\frac{\|x - y\|^2}{\ell^2}\right), \quad \text{with } \sigma = 1.5, \ell^2 = 1e-3.$$

552 For this experiment, a uniform triangular mesh of size  $h = 1/128$  is utilized. Using the  
 553 spectral decomposition method described in [37], we are able to obtain a realization  
 554 of  $\alpha_{\text{cont}}(x, w)$  at mesh vertices. The piecewise coefficient  $\alpha_\tau$  on an element  $\tau$  is then  
 555 defined as the average of  $\alpha_{\text{cont}}(x, w)$  at the three vertices. The distribution of  $\alpha$  with  
 556 a partition obtained from METIS [26] is shown in Figure 8. The contrast ratio in this  
 557 test case is nearly  $10^{10}$ . The coarse objects of rPB-BDDC(ce) when  $r = 10^2$  are also  
 558 illustrated.

559 In Table 5, we can see that, compared to the standard BDDC(ce) method, rPB-  
 560 BDDC(ce) and rPB-BDDC(e) preconditioners require much fewer iterations to con-  
 561 verge. They, however, have a larger coarse space. By adjusting the threshold for the  
 562 maximal contrast in each object, we can reduce the size of the coarse space while  
 563 maintaining a reasonably fast convergence. This is clearly illustrated in Table 5.

564 **5. Conclusions.** In this work, we have proposed a novel type of BDDC pre-  
 565 conditioner that are robust for heterogeneous problems with high contrast. The  
 566 underlying idea is to modify the continuity constraints enforced among subdomains  
 567 making use of the knowledge about the physical coefficients. In order to do that, we  
 568 rely on a physically motivated partition of standard coarse objects (corners, edges, and  
 569 faces) into coarse sub-objects. The motivation for that is the well-known robustness  
 570 of DD methods when there are only jumps of physical coefficients across the interface  
 571 between subdomains. All these ideas can also be used in the frame of FETI methods.

TABLE 5  
*Comparison of the iteration count in the log-normal test case.*

$r$	BDDC(ce)	rPB-BDDC(ce)			rPB-BDDC(e)		
		10	$10^2$	$5 \cdot 10^3$	10	$10^2$	$5 \cdot 10^3$
dim	49	488	284	239	204	127	105
# it.	77	16	25	28	25	29	33

572 In cases where the physical coefficient is constant in each coarse sub-object, we  
 573 are able to prove that the associated condition number can be bounded independent  
 574 of the number of the subdomains and the contrast of the physical coefficient. In other  
 575 words, the new preconditioner is scalable and robust for heterogeneous problems.

576 Apart from the new set of coarse objects and a new weighting operator, the (r)PB-  
 577 BDDC preconditioners are very much the same as the standard BDDC preconditioner.  
 578 As a result, the implementation of the new preconditioners involve a very simple  
 579 modification of the standard BDDC implementation. In all of our experiments, the  
 580 new preconditioners deliver fast, robust and contrast-independent convergence while  
 581 maintaining the simplicity of BDDC methods at a reasonable computational cost.  
 582 Compared to the other robust DD solvers for heterogeneous problems currently avail-  
 583 able, such as the ones in [25, 45, 25, 43, 44, 22, 23, 42, 47, 15, 49, 48, 28, 27, 29, 36, 24],  
 584 our new methods do not involve any type of eigenvalue or auxiliary problems.

585 For further work, we want to implement the new preconditioners in the extremely  
 586 scalable BDDC code in FEMPAR [3, 4, 5, 6]. The multilevel extension and the task-  
 587 overlapping implementation are particularly interesting in the (r)PB-BDDC case due  
 588 to generally larger coarse problem. With such extremely scalable implementation, we  
 589 are interested in applying our new preconditioners to realistic 3D problems, e.g., in  
 590 geoscience applications.

591

## REFERENCES

- 592 [1] A. ABDULLE, W. E. B. ENGQUIST, AND E. VANDEN-EIJNDEN, *The heterogeneous multiscale*  
 593 *method*, Acta Numer., 21 (2012), pp. 1–87.
- 594 [2] S. BADIA, A. F. MARTÍN, AND J. PRINCIPE, *Enhanced balancing Neumann-Neumann precon-*  
 595 *ditioning in computational fluid and solid mechanics*, International Journal for Numerical  
 596 Methods in Engineering, 96 (2013), pp. 203–230, <http://dx.doi.org/10.1002/nme.4541>.
- 597 [3] S. BADIA, A. F. MARTÍN, AND J. PRINCIPE, *Implementation and scalability analysis of balancing*  
 598 *domain decomposition methods*, Archives of Computational Methods in Engineering, 20  
 599 (2013), pp. 239–262, <http://dx.doi.org/10.1007/s11831-013-9086-4>.
- 600 [4] S. BADIA, A. F. MARTÍN, AND J. PRINCIPE, *A highly scalable parallel implementation of bal-*  
 601 *ancing domain decomposition by constraints*, SIAM Journal on Scientific Computing, 36  
 602 (2014), pp. C190–C218, <http://dx.doi.org/10.1137/130931989>.
- 603 [5] S. BADIA, A. F. MARTÍN, AND J. PRINCIPE, *On the scalability of inexact balancing domain*  
 604 *decomposition by constraints with overlapped coarse/fine corrections*, Parallel Computing,  
 605 50 (2015), pp. 1 – 24, <http://dx.doi.org/10.1016/j.parco.2015.09.004>.
- 606 [6] S. BADIA, A. F. MARTÍN, AND J. PRINCIPE, *Multilevel balancing domain decomposition at*  
 607 *extreme scales*, SIAM J. Sci. Comput., 38 (2016), pp. C22–C52, [http://dx.doi.org/10.](http://dx.doi.org/10.1137/15M1013511)  
 608 [1137/15M1013511](http://dx.doi.org/10.1137/15M1013511).
- 609 [7] S. BADIA AND H. NGUYEN, *Relaxing the roles of corners in bddc by perturbed formulation*, in  
 610 Domain decomposition methods in science and engineering XXIII, Lect. Notes Comput.  
 611 Sci. Eng., Springer, Heidelberg, accepted.
- 612 [8] S. BADIA AND H. NGUYEN, *Balancing domain decomposition by perturbation*, (submitted).
- 613 [9] S. C. BRENNER AND L. R. SCOTT, *The mathematical theory of finite element methods*, vol. 15  
 614 of Texts in Applied Mathematics, Springer, New York, third ed., 2008, <http://dx.doi.org/>

- 615 [10.1007/978-0-387-75934-0](https://doi.org/10.1007/978-0-387-75934-0).
- 616 [10] S. C. BRENNER AND L.-Y. SUNG, *BDDC and FETI-DP without matrices or vectors*, Computer  
617 Methods in Applied Mechanics and Engineering, 196 (2007), pp. 1429–1435, [http://dx.doi.  
618 org/10.1016/j.cma.2006.03.012](http://dx.doi.org/10.1016/j.cma.2006.03.012).
- 619 [11] T. F. CHAN AND T. P. MATHEW, *Domain decomposition algorithms*, Acta numerica, 3 (1994),  
620 pp. 61–143.
- 621 [12] C. R. DOHRMANN, *A Preconditioner for Substructuring Based on Constrained Energy Mini-  
622 mization*, SIAM Journal on Scientific Computing, 25 (2003), pp. 246–258, [http://dx.doi.  
623 org/10.1137/S1064827502412887](http://dx.doi.org/10.1137/S1064827502412887).
- 624 [13] C. R. DOHRMANN, *An approximate BDDC preconditioner*, Numerical Linear Algebra with  
625 Applications, 14 (2007), pp. 149–168, <http://dx.doi.org/10.1002/nla.514>.
- 626 [14] C. R. DOHRMANN AND O. B. WIDLUND, *A BDDC algorithm with deluxe scaling for three-  
627 dimensional  $H(\text{curl})$  problems*, Communications on Pure and Applied Mathematics, 69  
628 (2016), pp. 745–770, <http://dx.doi.org/10.1002/cpa.21574>.
- 629 [15] V. DOLEAN, F. NATAF, R. SCHEICHL, AND N. SPILLANE, *Analysis of a two-level Schwarz method  
630 with coarse spaces based on local Dirichlet-to-Neumann maps*, Comput. Methods Appl.  
631 Math., 12 (2012), pp. 391–414, <http://dx.doi.org/10.2478/cmam-2012-0027>.
- 632 [16] M. DRYJA, J. GALVIS, AND M. SARKIS, *BDDC methods for discontinuous Galerkin discretiza-  
633 tion of elliptic problems*, J. Complexity, 23 (2007), pp. 715–739, [http://dx.doi.org/10.1016/  
634 j.jco.2007.02.003](http://dx.doi.org/10.1016/j.jco.2007.02.003).
- 635 [17] M. DRYJA, M. V. SARKIS, AND O. B. WIDLUND, *Multilevel Schwarz methods for elliptic prob-  
636 lems with discontinuous coefficients in three dimensions*, Numer. Math., 72 (1996), pp. 313–  
637 348, <http://dx.doi.org/10.1007/s002110050172>.
- 638 [18] M. DRYJA, B. F. SMITH, AND O. B. WIDLUND, *Schwarz analysis of iterative substructuring  
639 algorithms for elliptic problems in three dimensions*, SIAM J. Numer. Anal., 31 (1994),  
640 pp. 1662–1694, <http://dx.doi.org/10.1137/0731086>.
- 641 [19] W. E, B. ENGQUIST, X. LI, W. REN, AND E. VANDEN-ELJNDEN, *Heterogeneous multiscale  
642 methods: a review*, Commun. Comput. Phys., 2 (2007), pp. 367–450.
- 643 [20] C. FARHAT, M. LESOINNE, P. LE TALLEC, K. PIERSON, AND D. RIXEN, *FETI-DP: a dual-  
644 primal unified FETI method-part I: A faster alternative to the two-level FETI method*,  
645 International Journal for Numerical Methods in Engineering, 50 (2001), pp. 1523–1544,  
646 <http://dx.doi.org/10.1002/nme.76>.
- 647 [21] C. FARHAT, M. LESOINNE, AND K. PIERSON, *A scalable dual-primal domain decomposition  
648 method*, Numerical Linear Algebra with Applications, 7 (2000), pp. 687–714, [http://dx.  
649 doi.org/10.1002/1099-1506\(200010/12\)7:7/8<687::AID-NLA219>3.0.CO;2-S](http://dx.doi.org/10.1002/1099-1506(200010/12)7:7/8<687::AID-NLA219>3.0.CO;2-S).
- 650 [22] J. GALVIS AND Y. EFENDIEV, *Domain decomposition preconditioners for multiscale flows in  
651 high-contrast media*, Multiscale Model. Simul., 8 (2010), pp. 1461–1483, [http://dx.doi.  
652 org/10.1137/090751190](http://dx.doi.org/10.1137/090751190).
- 653 [23] J. GALVIS AND Y. EFENDIEV, *Domain decomposition preconditioners for multiscale flows in  
654 high contrast media: reduced dimension coarse spaces*, Multiscale Model. Simul., 8 (2010),  
655 pp. 1621–1644, <http://dx.doi.org/10.1137/100790112>.
- 656 [24] M. J. GANDER, A. LONELAND, AND T. RAHMAN, *Analysis of a new harmonically enriched  
657 multiscale coarse space for domain decomposition methods*, Dec. 2015, [arXiv:1512.05285  
658 \[math.NA\]](https://arxiv.org/abs/1512.05285).
- 659 [25] I. G. GRAHAM, P. O. LECHNER, AND R. SCHEICHL, *Domain decomposition for multiscale PDEs*,  
660 Numer. Math., 106 (2007), pp. 589–626, <http://dx.doi.org/10.1007/s00211-007-0074-1>.
- 661 [26] G. KARYPIS AND V. KUMAR, *A fast and high quality multilevel scheme for partitioning irregular  
662 graphs*, SIAM J. Sci. Comput., 20 (1998), pp. 359–392 (electronic), [http://dx.doi.org/10.  
663 1137/S1064827595287997](http://dx.doi.org/10.1137/S1064827595287997).
- 664 [27] H. H. KIM AND E. T. CHUNG, *A BDDC algorithm with enriched coarse spaces for two-  
665 dimensional elliptic problems with oscillatory and high contrast coefficients*, Multiscale  
666 Model. Simul., 13 (2015), pp. 571–593, <http://dx.doi.org/10.1137/140970598>.
- 667 [28] A. KLAWONN, P. RADTKE, AND O. RHEINBACH, *FETI-DP methods with an adaptive coarse  
668 space*, SIAM Journal on Numerical Analysis, 53 (2015), pp. 297–320, [http://dx.doi.org/10.  
669 1137/130939675](http://dx.doi.org/10.1137/130939675).
- 670 [29] A. KLAWONN, P. RADTKE, AND O. RHEINBACH, *Adaptive coarse spaces for bddc with a trans-  
671 formation of basis*, in Domain Decomposition Methods in Science and Engineering XXII,  
672 T. Dickopf, J. M. Gander, L. Halpern, R. Krause, and F. L. Pavarino, eds., Springer Inter-  
673 national Publishing, 2016, pp. 301–309, [http://dx.doi.org/10.1007/978-3-319-18827-0\\_29](http://dx.doi.org/10.1007/978-3-319-18827-0_29).
- 674 [30] A. KLAWONN AND O. B. WIDLUND, *Dual-primal FETI methods for linear elasticity*, Commu-  
675 nications on Pure and Applied Mathematics, 59 (2006), pp. 1523–1572, [http://dx.doi.org/  
676 10.1002/cpa.20156](http://dx.doi.org/10.1002/cpa.20156).

- 677 [31] A. KLAWONN, O. B. WIDLUND, AND M. DRYJA, *Dual-primal FETI methods for three-*  
678 *dimensional elliptic problems with heterogeneous coefficients*, SIAM J. Numer. Anal., 40  
679 (2002), pp. 159–179 (electronic), <http://dx.doi.org/10.1137/S0036142901388081>.
- 680 [32] A. KLAWONN, O. B. WIDLUND, AND M. DRYJA, *Dual-primal FETI methods with face con-*  
681 *straints*, in Recent developments in domain decomposition methods (Zürich, 2001), vol. 23  
682 of Lect. Notes Comput. Sci. Eng., Springer, Berlin, 2002, pp. 27–40, [http://dx.doi.org/10.](http://dx.doi.org/10.1007/978-3-642-56118-4_2)  
683 [1007/978-3-642-56118-4\\_2](http://dx.doi.org/10.1007/978-3-642-56118-4_2).
- 684 [33] J. H. LEE, *A balancing domain decomposition by constraints deluxe method for Reissner-*  
685 *Mindlin plates with Falk-Tu elements*, SIAM J. Numer. Anal., 53 (2015), pp. 63–81, [http:](http://dx.doi.org/10.1137/130940669)  
686 [//dx.doi.org/10.1137/130940669](http://dx.doi.org/10.1137/130940669).
- 687 [34] J. LI AND O. B. WIDLUND, *FETI-DP, BDDC, and block Cholesky methods*, International  
688 Journal for Numerical Methods in Engineering, 66 (2006), pp. 250–271, [http://dx.doi.org/](http://dx.doi.org/10.1002/nme.1553)  
689 [10.1002/nme.1553](http://dx.doi.org/10.1002/nme.1553).
- 690 [35] J. LI AND O. B. WIDLUND, *On the use of inexact subdomain solvers for BDDC algorithms*,  
691 Computer Methods in Applied Mechanics and Engineering, 196 (2007), pp. 1415–1428,  
692 <http://dx.doi.org/10.1016/j.cma.2006.03.011>.
- 693 [36] S. LOISEL, H. NGUYEN, AND R. SCHEICHL, *Optimized schwarz and 2-lagrange multiplier methods*  
694 *for multiscale elliptic pdes*, SIAM Journal on Scientific Computing, 37 (2015), pp. A2896–  
695 A2923, <http://dx.doi.org/10.1137/15M1009676>.
- 696 [37] G. J. LORD, C. E. POWELL, AND T. SHARDLOW, *An Introduction to Computational Stochastic*  
697 *PDEs*, Cambridge Texts in Applied Mathematics, 2014.
- 698 [38] J. MANDEL, *Balancing domain decomposition*, Communications in Numerical Methods in En-  
699 gineering, 9 (1993), pp. 233–241, <http://dx.doi.org/10.1002/cnm.1640090307>.
- 700 [39] J. MANDEL AND C. R. DOHRMANN, *Convergence of a balancing domain decomposition by con-*  
701 *straints and energy minimization*, Numerical Linear Algebra with Applications, 10 (2003),  
702 pp. 639–659, <http://dx.doi.org/10.1002/nla.341>.
- 703 [40] J. MANDEL, B. SOUSEDÍK, AND C. DOHRMANN, *Multispace and multilevel BDDC*, Computing,  
704 83 (2008), pp. 55–85, <http://dx.doi.org/10.1007/s00607-008-0014-7>.
- 705 [41] T. P. A. MATHEW, *Domain decomposition methods for the numerical solution of partial dif-*  
706 *ferential equations*, vol. 61, Springer, 2008.
- 707 [42] F. NATAF, H. XIANG, V. DOLEAN, AND N. SPILLANE, *A coarse space construction based on*  
708 *local Dirichlet-to-Neumann maps*, SIAM J. Sci. Comput., 33 (2011), pp. 1623–1642, [http:](http://dx.doi.org/10.1137/100796376)  
709 [//dx.doi.org/10.1137/100796376](http://dx.doi.org/10.1137/100796376).
- 710 [43] C. PECHSTEIN AND R. SCHEICHL, *Analysis of FETI methods for multiscale PDEs*, Numer.  
711 Math., 111 (2008), pp. 293–333, <http://dx.doi.org/10.1007/s00211-008-0186-2>.
- 712 [44] C. PECHSTEIN AND R. SCHEICHL, *Analysis of FETI methods for multiscale PDEs. Part II:*  
713 *interface variation*, Numer. Math., 118 (2011), pp. 485–529, [http://dx.doi.org/10.1007/](http://dx.doi.org/10.1007/s00211-011-0359-2)  
714 [s00211-011-0359-2](http://dx.doi.org/10.1007/s00211-011-0359-2).
- 715 [45] R. SCHEICHL AND E. VAINIKKO, *Additive Schwarz with aggregation-based coarsening for elliptic*  
716 *problems with highly variable coefficients*, Computing, 80 (2007), pp. 319–343, [http://dx.](http://dx.doi.org/10.1007/s00607-007-0237-z)  
717 [doi.org/10.1007/s00607-007-0237-z](http://dx.doi.org/10.1007/s00607-007-0237-z).
- 718 [46] J. ŠÍSTEK, M. ČERTÍKOVÁ, P. BURDA, AND J. NOVOTNÝ, *Face-based selection of corners in 3D*  
719 *substructuring*, Math. Comput. Simulation, 82 (2012), pp. 1799–1811, [http://dx.doi.org/](http://dx.doi.org/10.1016/j.matcom.2011.06.007)  
720 [10.1016/j.matcom.2011.06.007](http://dx.doi.org/10.1016/j.matcom.2011.06.007).
- 721 [47] N. SPILLANE, V. DOLEAN, P. HAURET, F. NATAF, C. PECHSTEIN, AND R. SCHEICHL, *A robust*  
722 *two-level domain decomposition preconditioner for systems of PDEs*, C. R. Math. Acad.  
723 Sci. Paris, 349 (2011), pp. 1255–1259, <http://dx.doi.org/10.1016/j.crma.2011.10.021>.
- 724 [48] N. SPILLANE, V. DOLEAN, P. HAURET, F. NATAF, C. PECHSTEIN, AND R. SCHEICHL, *Abstract*  
725 *robust coarse spaces for systems of PDEs via generalized eigenproblems in the overlaps*,  
726 Numer. Math., 126 (2014), pp. 741–770, <http://dx.doi.org/10.1007/s00211-013-0576-y>.
- 727 [49] N. SPILLANE, V. DOLEAN, P. HAURET, F. NATAF, AND D. J. RIXEN, *Solving generalized eigen-*  
728 *value problems on the interfaces to build a robust two-level FETI method*, C. R. Math.  
729 Acad. Sci. Paris, 351 (2013), pp. 197–201, <http://dx.doi.org/10.1016/j.crma.2013.03.010>.
- 730 [50] A. TOSELLI AND O. WIDLUND, *Domain decomposition methods—algorithms and theory*, vol. 34  
731 of Springer Series in Computational Mathematics, Springer-Verlag, Berlin, 2005.
- 732 [51] X. TU, *Three-Level BDDC in Three Dimensions*, SIAM Journal on Scientific Computing, 29  
733 (2007), pp. 1759–1780, <http://dx.doi.org/10.1137/050629902>.
- 734 [52] O. B. WIDLUND AND C. R. DOHRMANN, *Domain Decomposition Methods in Science and Engi-*  
735 *neering XXII*, Springer International Publishing, Cham, 2016, ch. BDDC Deluxe Domain  
736 Decomposition, pp. 93–103, [http://dx.doi.org/10.1007/978-3-319-18827-0\\_8](http://dx.doi.org/10.1007/978-3-319-18827-0_8).
- 737 [53] Y. ZHU, *Domain decomposition preconditioners for elliptic equations with jump coefficients*,  
738 Numer. Linear Algebra Appl., 15 (2008), pp. 271–289, <http://dx.doi.org/10.1002/nla.566>.